中國文化大學工學院機械工程學系數位機電碩士班

碩士論文

Master's Thesis

Graduate Institute of Digital Mechatronic Technology
College of Engineering
Chinese Culture University

非線性動態系統之智慧型追蹤控制器

Intelligent Tracking Controller for Nonlinear Dynamic System

指導教授: 蘇國和教授
Advisor: Professor Kuo - Ho Su

研 究 生：蘇明煌
Graduate Student: To Minh Hoang

中華民國 102 年 6 月
June 2013

中 國 文 化 大 學

碩 士 學 位 論 文

Intelligent tracking controller for nonlinear dynamic system

研究生：蘇明煌
To Minh Hoang

經考試合格特此證明

口試委員：

指導教授：

所　　長：

口試日期：中華民國 102 年 06 月 20 日

ABSTRACT

In this thesis, an adaptive fuzzy PID sliding mode control (AFPIDSMC) scheme is proposed for a certain class of unknown nonlinear dynamical system. The proposed controller comprises of two types of controllers. One is fuzzy PID sliding-mode controller (FPIDSMC), which gives robust stability for system in the presence of parameter variations, uncertainties, and disturbances, and the other one is an adaptive tuner. The FPIDSMC acts as the main tracking controller, which is designed via a fuzzy system to mimic the merits of a PID sliding-mode controller (PIDSMC). While the adaptive tuner, which is derived in the sense of Lyapunov stability theorem, is utilized to adjust the parameter on-line for further assuring robust and optimal performance. In the proposed FPIDSMC, the fuzzy rule base is compact and only one parameter needs to be adjusted.

To verify its effectiveness and extend its application, the proposed AFPIDSMC is applied to path tracking for a control robots and to balance control for a two-wheel robot. In the first application, just only simulation results which are provided by MATLAB and whose advantages are presented in comparison with conventional AFSMC under the same environment. In the other application, the results are provided not only in simulation, but also in real world. The simulation results are also provided by MATLAB and are compared with conventional AFSMC while the experimental results are provided by using the E-NUVO platform.

ACKNOWLEDGEMENTS

First and foremost, I would like to thank to my advisor, Professor Kuo-Ho Su for his guidance, advice, inspiration and encouragements. The broad knowledge and serious academic attitude of my supervisors would benefit my life and always motivate me to never stop thinking, learning. He helped me concentrate to the topic, gave me the corrections by all his patience.

I also wish to express my sincere gratitude to Miss Shiu Wei-Jen, assistant of the Graduate Institute of Digital Mechatronic Technology, Chinese Culture University, for her kindness and enthusiasm of providing me the useful and quick information.

I owe special thanks to my classmates and laboratory mates for their supports and encouragements. Without their help, it is difficult for a foreign student like me can do anything as good as expected.

I will never be able to find words adequate to express my profound gratitude to my family, for their love, supports and sacrifices. Their encouragements are motivation for me to finish this thesis.

To Minh Hoang

June, 18th 2013

CONTENTS

LIST OF FIGURES

LIST OF TABLES

CHAPTER 1

INTRODUTION

Many physical systems are nonlinear and dynamic. Due to the highly nonlinear and uncertain characteristics within them, it is difficult to evaluate the appropriate control effort to track the desired trajectory. To this end, much research has been done to apply various approaches, such as nonlinear state feedback technique, sliding-mode control (SMC), fuzzy control (FC), fuzzy neural network control (FNNC), etc. Among these approaches, variable structure control with sliding mode, or SMC, is one of the effective nonlinear robust controllers since it provides system dynamics with an invariant property to uncertainties once the system dynamics are controlled in the sliding mode [1, 2]. Generally, the motion of the control system employing SMC can be divided into two phases. One is the reaching mode, and the other is the sliding mode. In the design procedure of SMC, the first step is to define a sliding surface. Then, design the control law such that the system trajectories move toward and stay on the sliding surface from any initial condition. The control phases before the state trajectory reaching the sliding surface are called the reaching mode, also called non-sliding mode. Once the system trajectory reaches the sliding surface, it stays on it and slides along the sliding surface to the origin of the phase plane. This is regarded as in the sliding mode. When the system trajectories enter the sliding mode, the control system can reject uncertainties and external disturbance, and the system dynamics can be specified by the pre-defined sliding surface. The most distinguished features of SMC include: (i) insensitive to variation in system parameters, (ii) external disturbances rejection ability, (iii) good transient performance, (iv) fast dynamic responses, and (v) easy realization. Consequently, SMC technique has been widely used to control nonlinear and uncertain systems. However, in practical application, the SMC suffers from two main drawbacks. One is that the requirement of the uncertainty bound in SMC may be difficult to obtain in advance for some applications. Other is that, because the magnitude of uncertainty bound is unknown, the large switching control gain is always chosen in order to guarantee the system stability. Unfortunately, this causes high-frequency control chattering, which may result in unforeseen instability and deterioration of the system performance.

On the other hand, FC has supplanted conventional technologies in many applications. In the conventional control theory, most of the control problems are usually solved by mathematical tools based on the system models. But in the real world, there are many complex industrial processes whose accurate mathematical models are not available or difficult to formulate. One major feature of fuzzy system is its ability to express the amount of ambiguity in human thinking. Thus, when the mathematical model of the process does not exist, or exists but with uncertainties, FC is an alternative way to deal with the unknown process [3, 4]. But there exists an error between the exact nonlinear system and the approximated fuzzy model. Therefore, an adaptive fuzzy control system has been proposed to incorporate with the expert information systematically and the stability can be guaranteed by theoretical analysis. The most important advantage of the adaptive fuzzy control compared with other conventional adaptive control methods is that an adaptive fuzzy controller is capable of incorporating linguistic fuzzy information from human operators and has certain learning or training capability. In Wang and Mendel’s works, fuzzy logic systems (center average defuzzifier, product-inference rule, singleton fuzzifier, and Gaussian membership function) are capable of uniformly approximating any nonlinear function over compact input space; that is, any nonlinear system can be modeled by the fuzzy logic systems. Especially, Wang utilized the general error dynamics of adaptive control to design the adaptive fuzzy controller.

Even in consideration with the advantages of Adaptive Fuzzy Control, there still existed the problem that the huge amount of fuzzy rules for high order systems makes the analysis complex. Therefore, much attention has focused on the combination between FC and SMC. In the past decade, the nonparametric scheme fuzzy sliding mode control (FSMC) was proposed which retains the favorable aspects of SMC but improves robustness by merging the SMC controller into the IF-THEN linguistic rule, using the expert's experience of systematic tuning scheme as well. To further achieve satisfactory response, adaptive FC (AFC) and/or adaptive FSMC (AFSMC) schemes have been developed [7-9] for nonlinear dynamic system. With the dynamic adaptation mechanism, the parameters can be automatically adjusted. Thus, with the final combination between SMC and AFC, the controller not only maintains the advantages, but also overcomes the disadvantages of each proposed method.

However, the gradual increasing estimated upper bound, existed in some announced works, might induce the control effort into saturation and excite unstable system dynamics in some conditions [5, 6]. To improve this drawback, a PID sliding surface is adopted and incorporated into fuzzy inference engine to strengthen its anti-disturbance ability in this thesis. First, the PID sliding surface is chosen. Then, a fuzzy rule base is applied to calculate the total control effort. In the last, an adaptive tuner is adopted to the controller to adjust parameters. However, the number of parameters needed adjustment is generally deemed large such that the response time is lengthened. To improve this phenomenon, another objective of this thesis is to research a novel scheme which possesses compact fuzzy rule base and only one parameter needs to be adjusted.

Thus, this thesis suggests a powerful adaptive fuzzy PID sliding mode controller (AFPIDSMC) to solve the problems in tracking controller. The main advantages of controller are better performance is usually achieved because the PID sliding function is more effectiveness with disturbance and uncertainties than the original sliding function.

This thesis is organized as follows: Chapter 2 presents some basic principles, including FC and SMC. In Chapter 3, the design proposed AFPIDSMC for a general nonlinear dynamic system is presented. Two applications are presented with the simulation and experimental results to illustrate the advantages of the proposed method in Chapter 4. These applications are: path tracking control for wheel robot - with simulation results in MATLAB, and balance control for t wheeled robot – with simulation results in MATLAB and experimental results are provided by practicing with two-wheeled E-NUVO robot. Finally, the conclusions are presented in Chapter 5.

CHAPTER 2

BASIC PRINCIPLES

2.1. Fuzzy control system

The concept of Fuzzy Logic (FL) was conceived by Lotfi Zadeh. FL and FC theories added a new dimension to control systems engineering in the early 1970s. From its beginnings as mostly heuristic, more recent and rigorous approaches to fuzzy control theory have helped make it integral part of modem control theory and produced many exciting results. There are four important elements in the fuzzy logic controller system structure which are fuzzifier, rule base, inference engine and defuzzifier. Details of the fuzzy logic controller system structure can be seen in Figure 2.1 below. Firstly, a crisp set of input data are gathered and converted to a fuzzy set using fuzzy linguistic variables, fuzzy linguistic terms and membership functions. This step also known as fuzzification. Afterwards, an inference is made base on a set of rules. Lastly, the resulting fuzzy output is mapped to a crisp output using the membership functions, in the defuzzification step.

Figure 2.1 shows a fuzzy logic control system in a closed loop control. The plant output is denoted by e(t), the input is denoted by u(t), and the reference input to the fuzzy controller is denoted by r(t) .

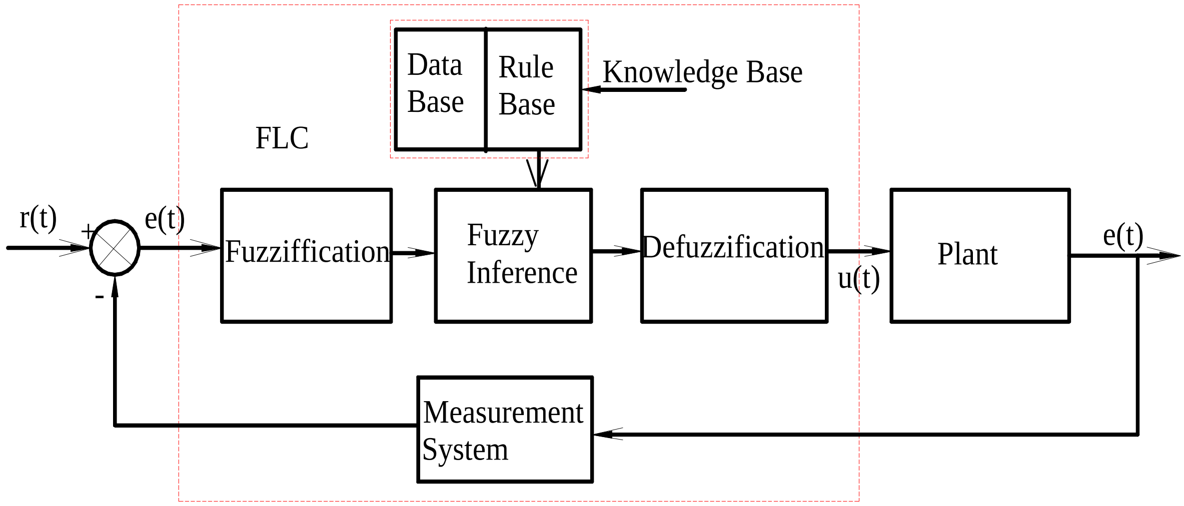

Figure 2. 1. Fuzzy logic control system

2.1.1. Fuzzification

Fuzzification is a process of making a crisp quantity fuzzy. Before this process is taken in action, the definition of the linguistic variables and terms is needed.

Linguistic variables are the input or output variables of the system whose values are words or sentences from a natural language, instead of numerical values. A linguistic variable is generally decomposed into asset of linguistic terms. Next, to map the non-fuzzy input or crisp input data to fuzzy linguistic terms, membership functions is used. In other words, a membership function as shown in Figure 2.2 is used to quantify a linguistic term. Note that, an important characteristic of fuzzy logic is that a numerical value does not have to be fuzzified using only one membership function meaning, a value can belong to multiple sets at the same time [3]. There are different forms or shapes of membership functions such as Triangular, Gaussian, Ttrapezoidal, Generalized Bell and Sigmoidal. Figure 2.2 shows the different types of membership function shape.

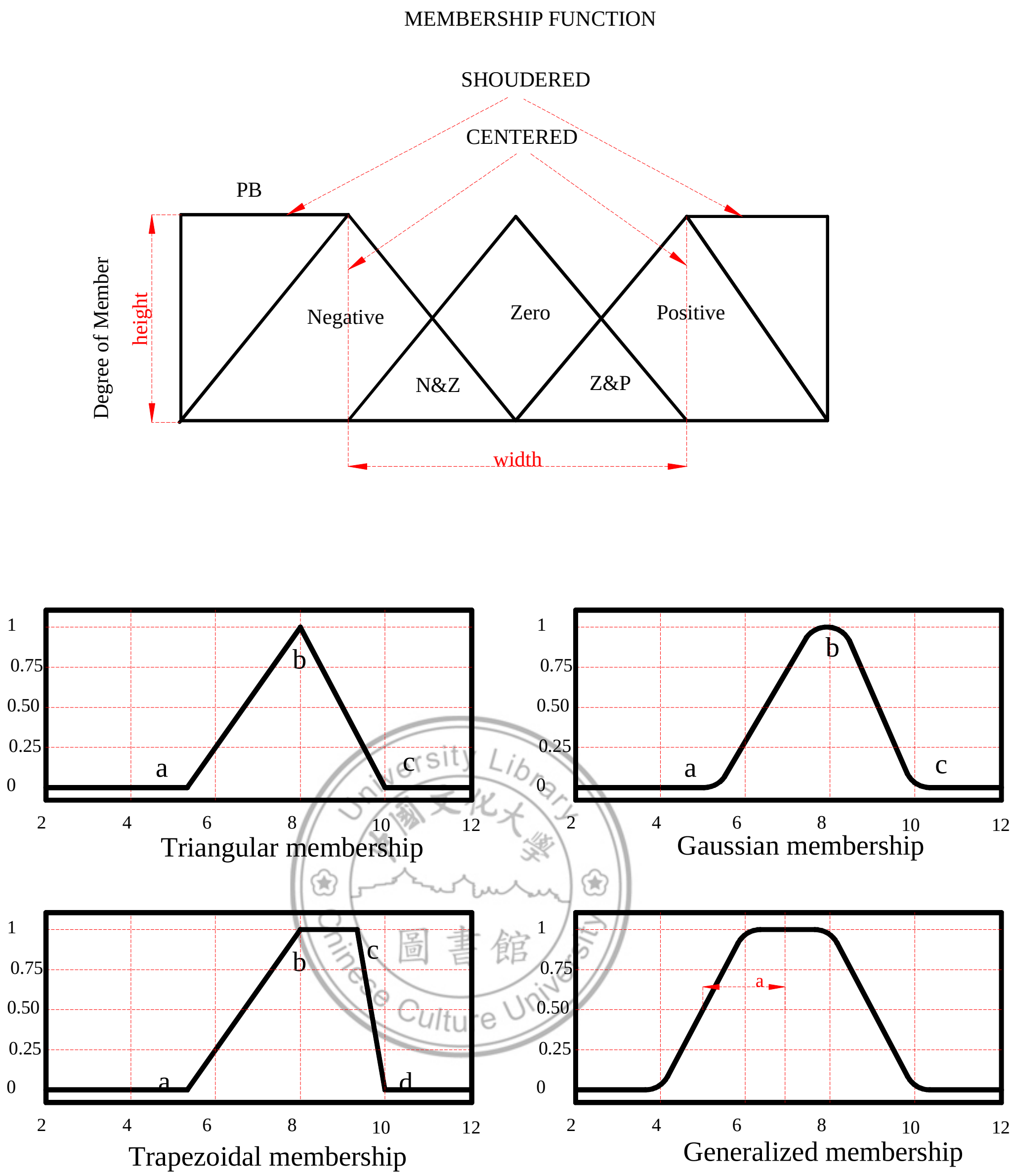

Figure 2. 2. The features of a membership function

2.1.2. Rule base

In a fuzzy logic control system, a rule base is constructed to control the output variable. A fuzzy rule is a simple IF-THEN rule with a condition and conclusion. It can be represented by the matrix table. The premise variables *error* and *change in error* are laid out along the axes, and the conclusions are inside the table. The most prominent connective is the '*and*' connective, often implemented as multiplication instead of minimum. For examples 'If *error* is Neg and *change in error* is Pos then *control* is Zero.

Control		Change in Error		
		Neg	Zero	Pos
Error	Neg	NB	NM	Zero
	Zero	NM	Zero	PM
	Pos	Zero	PM	PB

Table 2. 1. Example of rule base

2.1.3. Rules of inference

In general, inference is a process of obtaining new knowledge through existing knowledge. In the context of fuzzy logic control system, it can be defined as a process to obtain the final result of combination of the result of each rule in fuzzy value. There are many methods to perform fuzzy inference method and the most common two of them are Mamdani and Takagi-Sugeno-Kang method. Mamdani method was proposed by Ebrahim Mamdani as an attempt to control a steam engine and boiler in 1975. It is based on Lofti Zadeh's 1973 paper on fuzzy algorithms for complex system and decision processes [3]. This method uses the minimum operation as a fuzzy implication and the max-min operator for the composition. Suppose a rule base is given in the following form:

IF input x = A AND input y = B THEN output z = C

After the aggregation process, there is a fuzzy set for each output variable that needs defuzzification. It is possible and in many cases much more efficient, to use a single spike as the output membership functions rather than a distributed fuzzy set. This is sometimes known as a singleton output membership function. It enhances the efficiency of defuzzification process because it greatly simplifies the computation required by the more general Mamdani method, which finds the *centroid* of two dimensional function.

Meanwhile, Takagi-Sugeno-Kang method was introduced in 1985 and it is similar to the Mamdani method in many aspects. The first two parts of fuzzy inference processes which are fuzzifying the inputs and applying the fuzzy operator are exactly the same. But, the main difference is that the Takagi-Sugeno-Kang output membership function is either linear or constant. A typical rule in Takagi-Sugeno-Kang fuzzy model has the form as follows:

IF input 1 = x AND input 2 = y THEN output z = ax + by + c

	Mamdani	Sugeno
Similarity	The antecedent parts of the rules are the same	
Difference	The consequent parts are fuzzy sets	The consequent parts are singletons (single spikes) or mathematical equation
Advantages	1. Easily understandable by a human expert. 2. Simpler to formulate rules 3. Proposed earlier and commonly used	1. More effective computationally. 2. More convenient in mathematical analysis and in system analysis. 3. Guarantees continuity of the output surface

Table 2. 2. Mamdani and Sugeno fuzzy method

2.1.4. Defuzzification

After the inference step, the overall result is a fuzzy value. This result should be defuzzified to obtain a final crisp output. This is the purpose of the defuzzification component of a fuzzy logic controller system. Defuzzification is performed according to the membership function of the output variable. There are many different methods for defuzzification such as Centroid of Gravity (COG), Mean of Maximum (MOM), Weighted Average, Bisector of Area (BOA), First of Maxima and Last of Maxima. There is no systematic procedure for choosing a good defuzzification strategy, but the selection of defuzzification procedure is depends on the properties of the application [3].

Centroid of Gravity (COG) is the most frequently used and the most prevalently and physically appealing of all defuzzification methods. The basic equation of Centroid of Gravity (COG) as below:

$$u_0 = \frac{\int_u \mu_u(u) u du}{\int_u \mu_u(u) du} \tag{2.1-1}$$

where u_0 is control output obtained by using Centroid of Gravity (COG) defuzzification method.

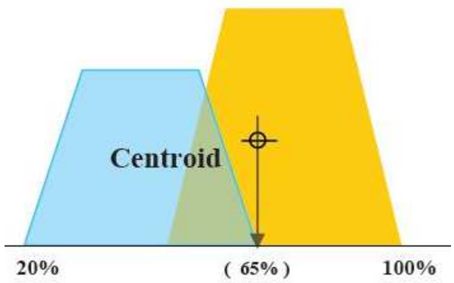

Figure 2. 3. Centroid of Gravity (COG) defuzzification method.

2.1.5. Advantages and disadvantages of fuzzy logic controller

a) Advantages:

Fuzzy logic is not only the way to reason with ambiguous concepts but is seems to be the most apt to function approximation in control engineering. From the previous considerations, some of the most important advantages the use of fuzzy logic can entail to control system design are here detailed:

- Flexible, intuitive knowledge base design control and supervision speak the same language.
- Convenient user interface, easier end-user interpretation when the final user is not a control engineer.
- Easy computation. Widely available toolboxes and dedicated integrated circuits.
- Validation: Consistency, redundancy and completeness can be checked in rule-bases (knowledge acquisition supervision). That could speed up automated learning and improve user interpretability.
- Ambiguousness: Fuzzy logic is a "natural" way of expressing uncertain information. Research must be done in reasoning with incompleteness, i.e., concluding different actions depending on the possibility or necessity og certain plant situations.
- Combine regulation algorithms and logic reasoning, allowing for integrated control schemas.
- FLC can incorporate a conventional design (PID, state feedback) and fine-tune it to certain plant nonlinearities due to universal approximation capabilities.

b) Disadvantages:

- Many (localized) parameters: Manual local tuning is tedious but it can be an advantage for automated learning algorithms. A much simpler global description may exits, being hidden by too detailed local descriptions. As in most modeling situations, the compromise between accuracy and readability may be present.

- Many (unclear) options: thousands of different fuzzy system configurations may arise depending on conjunction, disjunction, implication and defuzzification choices. Some of the alternatives even stem from the root interpretation of the meaning of fuzziness.
- For the high order dynamic system or the complex system, the number of rules is very large. Thus, the controller will be complex and it is difficult to design as well as to practice in real world.

2.2. Sliding mode based approaches

A sliding mode controller is suitable for a specific class of nonlinear systems. This is applied in the presence of modeling inaccuracies, parameter variation and disturbances, provided that the upper bounds of their absolute values are known. Modeling inaccuracies may come from certain uncertainty about the plant (e.g. unknown plant parameters), or from the choice of a simplified representation of the system dynamic. Sliding mode controller design provides a systematic approach to the problem of maintaining stability and satisfactory performance in presence of modeling imperfections [2]. The sliding mode control is especially appropriate for the tracking control of motors, robot manipulators whose mechanical load change over a wide range. Induction motors are used as actuators which have to follow complex trajectories specified for manipulator movements. Advantages of sliding mode controllers are that it is computationally simple compared adaptive controllers with parameter estimation and also robust to parameter variations. The disadvantage of sliding mode control is sudden and large change of control variables during the process which leads to high stress for the system to be controlled. It also leads to chattering of the system states [2].

Sliding mode is also called sliding error surface or a hyper surface that is a function of observer error function. Once the tracking error trajectories have reached this hyper surface, the error-based action makes the observation errors “slide” to zero. The sliding mode based tracking controller is derived from sliding error surface. Sliding mode technique has been investigated.

Sliding mode based approaches were used to designed a tracking control law according to a time varying sliding surface of errors S(t), defined as:

$$S(X_e, t) = X_e + (\frac{dX_e}{dt} + \lambda)^{n-1}, \lambda > 0, n = 1,2,.... \quad (2.2\text{-}1)$$

where λ is a positive constant and $X_e = X - X_d$. The variable X is an n-dimension vector in the state space denoted as R^n .

Figure 2.4 shows an example trajectory of a system under sliding mode control. The sliding surface is described by S = 0 and the sliding mode along the surface commences after the finite time when system trajectories have reached the surface. In the theoretical description of sliding modes, the system stays confined to the sliding surface and need only be viewed as sliding along the surface. However, real implementations of sliding mode control approximate this theoretical behavior with a high-frequency and generally non-deterministic switching control signal that causes the system to "chatter" in a tight neighborhood of the sliding surface [2]. This chattering behavior is evident in Figure 2.4, which chatters along the S = 0 surface as the system asymptotically approaches the origin, which is an asymptotically stable equilibrium of the system when confined to the sliding surface. In fact, although the system is nonlinear in general, the idealized (i.e., non-chattering) behavior of the system in Figure 2.4 when confined to the S = 0 surface is an LTI system with an exponentially stable origin.

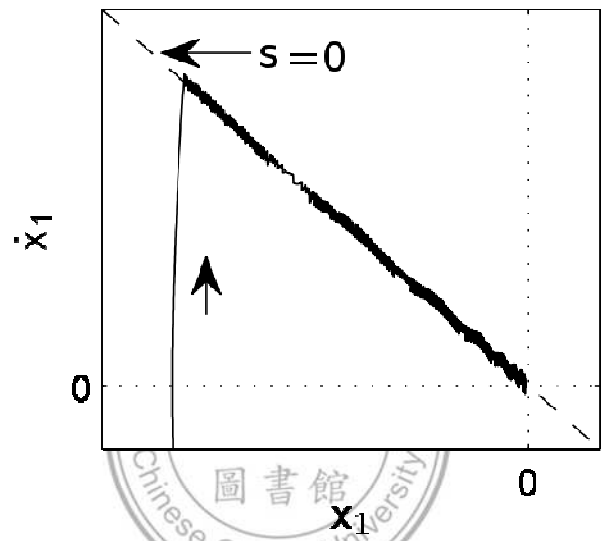

Figure 2. 4. Phase plane trajectory of $S = x_1 + \dot{x}_1$

The chosen control laws have to satisfy the sliding and the initial conditions. The sliding condition is defined as

$$\frac{1}{2}\frac{d}{dt}S^2(X_e, t) \le -\eta\,|\,S\,|. \tag{2.2-2}$$

where η is a positive constant value, and the initial condition is defined as

$$X_e\,|_{t=0} = 0 \tag{2.2-3}$$

Therefore, the designed control laws have to be discontinuous across the sliding surface, which leads to chattering. This might be the cause of the speed jump (or the speed discontinuousness) that is impossible in the real world because the time derivative of the velocity approaches to infinity [2].

Sliding observer based tracking controllers replace the desired state with the estimated state. The observation error is given as the difference between the process output and the estimation of the process output. The sliding observer was used to design the tracking controllers. Although the sliding observer has better results than Kalman Filter, it has the same problem as the sliding mode based controller. Furthermore, both sliding-mode based controller and sliding-observer based controller have to require a good dynamics model of the system and completely know the inaccuracies and uncertainties in the model that is impossible in the real world.

CHAPTER 3

TRACKING CONTROLLER FOR NONLINEAR DYNAMIC SYSTEM

3.1. Description of nonlinear system

Consider an *n*th – order nonlinear dynamic system of the form:

$$\begin{aligned} x^{(n)} &= f(\underline{x}) + g(\underline{x})u + d(t) \\ y &= x \end{aligned} \tag{3.1-1}$$

where:

$f(\underline{x})$ and $g(\underline{x})$ unknown continuous functions, $g(\underline{x})$ is positive and invertible

$u \in \Re$ control effort

$y \in \Re$ output of the system

$\underline{x} \in \Re^n$ state vector of the system

d(t) unknown external disturbance

And $\underline{x} = (x_1, x_2, x_3, ..., x_n)^T = (x, \dot{x}, \ddot{x}, ..., x^{(n-1)})^T \in \Re^n$, which is assumed to be measurable .

In order for (3.1-1) to be controllable, it is required that $g(\underline{x})$ for $\underline{x}$ in certain controllability region $U_c \subset \Re^n$ and that *d(t)* has upper bound *D*; that is, |*d(t)*| ≤ *D*. The detailed descriptions of each control part are exhibited in the following subsections.

3.2. FPIDSMC design

The control problem is to obtain the state $\underline{x}$ to track a desired state vector $\underline{x}_d = (\underline{x}_d, \dot{\underline{x}}_d, \ddot{\underline{x}}_d, ..., \underline{x}_d^{(n-1)})^T \in R^n$. The tracking error is defined as

$$\underline{e} = \underline{x} - \underline{x}_d = (e, \dot{e}, \ddot{e}, ..., e^{(n-1)})^T \tag{3.2-1}$$

Now, a PID sliding surface is designed as following scalar equation:

$$S = \underline{a}^T \dot{\underline{e}} + \underline{b}^T \underline{e} + \underline{h}^T \int \underline{e} d\tau \tag{3.2-2}$$

where: $\underline{a} = (a_0, a_1, a_2, ..., a_{n-1})^T$, $\underline{b} = (b_0, b_1, b_2, ..., b_{n-1})^T$ and $\underline{h} = (h_0, h_1, h_2, ..., h_{n-1})^T$.

All the elements of following series sequence must be real number and satisfy the Routh - Herwitz condition:

$$(h_0, b_0 + h_1, a_0 + b_1 + h_2, a_1 + b_2 + h_3, ..., a_{n-3} + b_{n-2} + h_{n-1}, a_{n-2} + b_{n-1}, a_{n-1})$$

The control effort as the solution of $S = 0$ without considering the uncertainties is to achieve the desired performance under nominal model, and it is referred to as nominal control effort as follows

$$u_0 = \frac{1}{g(\underline{x})}[-K + x_d^{(n)} - f(\underline{x})] \tag{3.2-3}$$

where: $K = h_0 \int e d\tau + (b_0 + h_1)\dot{e} + \sum_{i=0}^{n-3} (a_i + b_{i+1} + h_{i+2}) e^{(i)} + (a_{n-2} + b_{n-1}) e^{(n-1)}$ (3.2-4)

with consideration $a_{n-1} = 1$.

However, if uncertainties occur then the nominal control effort cannot guarantee the desired performance and an auxiliary control effort should be added to eliminate the effect of the unpredictable perturbation. Let the sliding surface, *S*, be the input linguistic variable of the fuzzy logic, and the total control effort, *u*, be the output linguistic variable. The associated fuzzy sets for *S* and *u* are designed as follow:

For *S*: P (Positive), N (Negative), Z (zero).

For *u*: DU (Decreased control effort), NU (Nominal control effort), IU (Increased control effort).

Then, the fuzzy linguistic rule base involved can be summarized as

Rule 1: If *S* is P then u is DU

Rule 2: If *S* is Z then u is NU

Rule 3: If *S* is N then u is IU

The triangular membership functions and center average defuzzification method are adopted in the proposed path following inference mechanism. The membership functions of *S* and *u* are depicted in Fig. 3.1, respectively. Thus, the total control effort can be obtained as

$$\hat{u} = w_1(u_0 - c) + w_2 u_0 + w_3(u_0 + c) \tag{3.2-5}$$

where $u_0 - c$, and $u_0 + c$ are the center of the membership function DU, NU and IU, respectively, in which $c > 0$ is the translation width; $0 \le w_1 \le 1$, $0 \le w_2 \le 1$, and

$0 \le w_3 \le 1$ are the firing strength of Rule 1, 2 and 3, respectively. Note that, since the fuzzy sets for S are triangular membership functions and the relation $w_1 + w_2 + w_3 = 1$ is valid, equation (3.2-5) can be written as

$$\hat{u} = u_0 + c(w_1 - w_3) \tag{3.2-6}$$

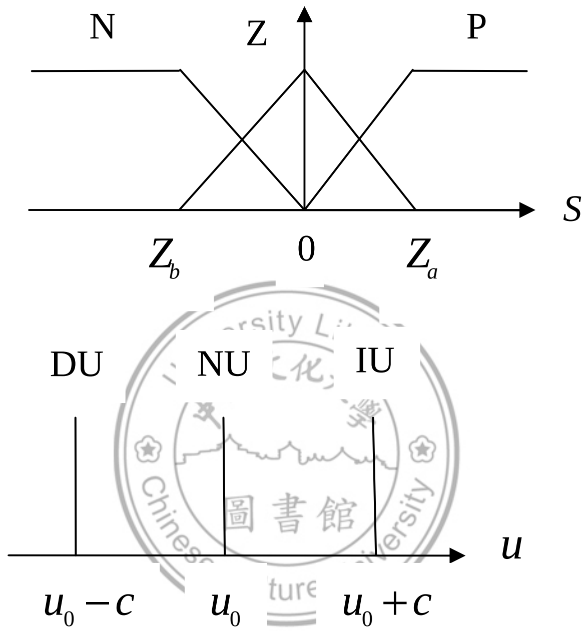

Figure 3. 1. Membership functions of S and u

Theorem (Lyapunov's second method stability)*: Consider a function* $V(x): R^n \to R$ *such that:*

- $V(x) \ge 0$ *with equality if and only if* $x = 0$ *(positive definite)*
- $\dot{V}(x) = \dfrac{d}{d(t)} V(x) \le 0$ *with equality if and only if* $x = 0$ *(negative definite)*

Then $V(x)$ is called a Lyapunov function candidate and the system is asymptotically stable in the sense of Lyapunov.

Consider a Lyapunov function candidate :

$$V_a = \int sign(S) S d\tau = \int |S| d\tau \tag{3.2-7}$$

where S is the PID sliding surface. Differentiating V with respect to time, we can obtain:

$$\begin{aligned} \dot{V}_a &= sign(S)S = sign(S)[K + e^{(n)}] \\ &= sign(S)[K + f(\underline{x}) + g(\underline{x})\hat{u} + d(t) - x_d^{(n)}] \end{aligned} \tag{3.2-8}$$

Substituting equations (3.2-3) and (3.2-6) into equation (3.2.8) yields:

$$\begin{aligned} \dot{V}_a &= sign(S)[g(\underline{x})c(w_1 - w_3) + d(t)] \\ &= sign(S)g(\underline{x})c(w_1 - w_3) + sign(S)d(t) \\ &\le sign(S)g(\underline{x})c(w_1 - w_3) + |d(t)| \end{aligned} \tag{3.2-9}$$

From the relationships among S, w_1 and w_3, following conditions can be further concluded.

Condition 1: **If** $S > 0$ **then** $w_1 = 0, w_3 > 0 \Rightarrow sign(S)(w_1 - w_3) = w_1 - w_3 < 0$

Condition 2: **If** $S < 0$ **then** $w_3 = 0, w_1 > 0 \Rightarrow sign(S)(w_1 - w_3) = -(w_1 - w_3) < 0$

Thus: $$sign(S)(w_1 - w_3) = -|w_1 - w_3| \tag{3.2-10}$$

and equation (3.2-9) can be rewritten as follows

$$\begin{aligned}\dot{V}_a &\le -g(\underline{x})c\,|w_1 - w_3| + |d(t)| \\ &= -[g(\underline{x})c\,|w_1 - w_3| - D]\end{aligned} \tag{3.2-11}$$

If the following inequality

$$g(\underline{x})c\,|w_1 - w_3| \ge D \tag{3.2-12}$$

holds, then the sliding condition $\dot{V}_a \le 0$ can be satisfied. As a result, the asymptotic stability can be assured under some specific conditions.

3.3. Adaptive tuner design

Although the performance of the system can be improved after using the fuzzy rule base, but it still be difficult to choose the optimal parameter of membership function. To solve this problem, a dynamic adaptation mechanism was added into the FPIDSMC. In this study, term *c* is designed as a tunable parameter and the Lyapunov stability theorem is utilized to derive the adaptive law. Now, equation (3.2-6) can be modified as

$$\hat{u} = u_0 + \hat{c}(w_1 - w_3) \tag{3.3-1}$$

where $\hat{c}$ is the estimated value of parameter *c*. Assume c^* is the optimal value of *c* and $\tilde{c} = \hat{c} - c^*$ is the estimated error.

To derive the adaptive law, following Lyapunov function candidate is considered:

$$V_b = \int |S|\,d\tau + \frac{g(\underline{x})\alpha\tilde{c}^2}{2} \tag{3.3-2}$$

where α is a positive constant. Differentiating V_b with respected to time, we can obtain:

$$\dot{V}_b = sign(S)S + g(\underline{x})\alpha\tilde{c}\dot{\hat{c}}$$

$$
\begin{aligned}
&= -[g(\underline{x})\hat{c}\,|\,w_1 - w_3\,| - d(t)] + g(\underline{x})\alpha\tilde{c}\dot{\hat{c}} \\
&= -g(\underline{x})\,|\,w_1 - w_3\,|\,[\hat{c} - c^* + c^* - \frac{d(t)}{g(\underline{x})\,|\,w_1 - w_3\,|}] + g(\underline{x})\alpha\tilde{c}\dot{\hat{c}} \\
&= -g(\underline{x})\,|\,w_1 - w_3\,|\,[\tilde{c} + \frac{D}{g(\underline{x})\,|\,w_1 - w_3\,|} + \varepsilon - \frac{d(t)}{g(\underline{x})\,|\,w_1 - w_3\,|}] + g(\underline{x})\alpha\tilde{c}\dot{\hat{c}} \\
&\le -g(\underline{x})\,|\,w_1 - w_3\,|\,[\tilde{c} + \varepsilon] + g(\underline{x})\alpha\tilde{c}\dot{\hat{c}}
\end{aligned}
$$

$$= -g(\underline{x})\,|\,w_1 - w_3\,|\,\varepsilon + g(\underline{x})\tilde{c}[\alpha\dot{\hat{c}} - |\,w_1 - w_3\,|] \qquad (3.3\text{-}3)$$

where ε is a positive constant and ε is as small as possible

If the adaption law for *c* parameter is designed as

$$\dot{\hat{c}} = \frac{|\,w_1 - w_3\,|}{\alpha} \qquad (3.3\text{-}4)$$

where α is trade-off problem of controller, then equation (3.3-3) becomes:

$$\dot{V}_b \le -g(\underline{x})\,|\,w_1 - w_3\,|\,\varepsilon \qquad (3.3\text{-}5)$$

According to $g(\underline{x})\,|\,w_1 - w_3\,|\,\varepsilon > 0$, one can obtain that $\dot{V}_b \le 0$. This means that the system will be still stable if the adaptation law for parameter *c* is tuned by equation (3.3-4). The overall scheme of the proposed AFPIDSMC tracking system is depicted in Fig. 3.2.

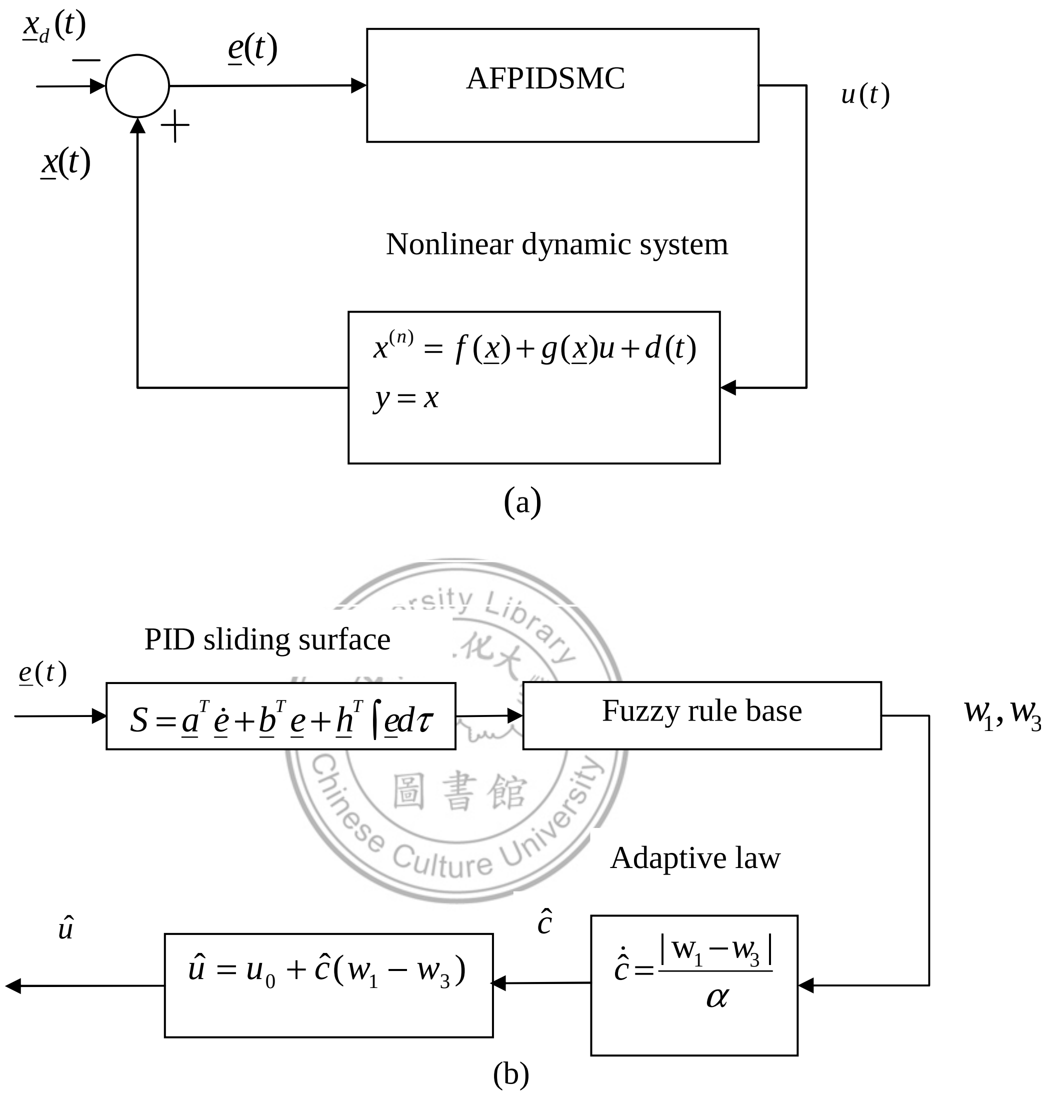

Figure 3. 2. Overall scheme of the proposed AFPIDSMC tracking system

(a) Whole control system; (b) AFPIDSMC strategy

CHAPTER 4

SIMULATION AND EXPERIMENTAL RESULTS

In order to verify the proposed fuzzy PID sliding mode control, we give the simulations and experiments to obtain the satisfactory result. In the first example, the objective is to drive the wheel robot to follow a sine-wave trajectory as well and compare with AFSMC method. The results are provided by simulation in MATLAB. In the second example, the control objective is to balance the inverted pendulum. The results in this example are provided by simulation and experiment, in comparison with Fuzzy control method as well.

4.1. Path tracking for wheel robot

Nowadays, the wheeled robot has been finding wide application in industrial, commercial and residential environments; however, the accurate model of the dynamic motion equation is difficult to establish or identify for designing an optimal path tracking controller. Also, the path tracking performance of a wheeled robot is influenced by system uncertainties, such as mechanical parameter variation, steering environment, payload changes, unstructured uncertainty due to nonideal motor control in transient state, unmodelled dynamics, etc. In recent years, the AFSMCs have been adopted to steer the wheeled robot path [10-15]. However, if the plant knowledge or control information is incomplete seriously then the load of adaptive algorithm will be heavy, the response time will be lengthened and the tracking error will be large. To verify the effectiveness of the proposed control scheme, the AFPIDSMC is applied to the path tracking of a wheeled robot. The design procedures and theoretical analyses of the proposed control system are described in detail. To compare with other AFSMC scheme [15], the same steering environment is employed in the simulation. The results are provided to demonstrate the effectiveness of the proposed AFPIDSMC tracking system and its advantages.

Figure 4. 1. Pioneer robot

4.1.1. Kinematic dynamics of wheeled robot

The structure and parameters of a wheeled robot is shown in Fig.4.2; the kinematic equation of a wheeled robot can be represented as [16]

$$\begin{aligned} \dot{x} &= \frac{r\cos(\phi)}{2}(V_R + V_L) \\ \dot{y} &= \frac{r\sin(\phi)}{2}(V_R + V_L) \\ \dot{\phi} &= \frac{r}{2\eta}(V_R - V_L) \end{aligned} \tag{4.1-1}$$

where $\dot{x}$, $\dot{y}$, r, η, ϕ, V_R, and V_L denote the proceeding distance change in x-axis, y-axis, radius of wheel, half width of the chassis, proceeding angle of robot's heading direction, speed of right and left wheel respectively.

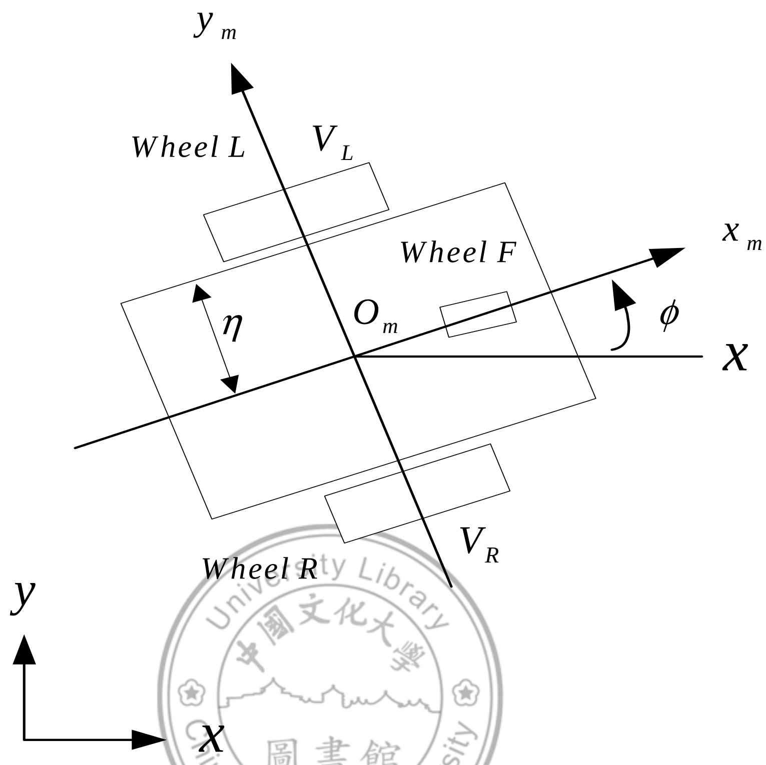

Figure 4. 2. Structure and parameters of a wheeled robot

Consider equation (4.1-1) parametric variation, computing error due to unpredicted uncertainties for the actual wheeled robot

$$\begin{aligned} \dot{x} &= \overline{r}\cos(\overline{\phi})V_R - \overline{\eta}\cos(\overline{\phi})\dot{\overline{\phi}} + L_x \\ \dot{y} &= \overline{r}\sin(\overline{\phi})V_L + \overline{\eta}\sin(\overline{\phi})\dot{\overline{\phi}} + L_y \end{aligned} \qquad (4.1\text{-}2)$$

where L_x and L_y are the total uncertainty for *x*-axis and *y*-axis, respectively. Here the bound of the total uncertainty is assumed to be given; that is,

$$|L_x| < \rho, \quad |L_y| < \rho \tag{4.1-3}$$

where ρ is a given positive constant.

4.1.2. AFPIDSMC path tracking

The purpose of the path tracking system is to make the robust following to the desired path. The path tracking error may occur due to command error, sluggish transformation, variation of robot parameters, friction, bumpy condition or transmitting efficiency etc. To track the prescribed path smoothly, a robust tracking scheme must be embedded into controller to calibrate the proceeding path simultaneously. In Elie *et al*. [17] and Jang [18], the angle and distance errors were fed into conventional controllers to modify robot's proceeding path. However, the tracking performance was not satisfactory because there existed with the chattering phenomenon and longer response time. In the past four decades, fuzzy systems have supplanted conventional technologies in many applications, especially in control systems. One major feature of fuzzy logic is its ability to express the amount of ambiguity in human thinking. Thus, it is appropriate to apply fuzzy logic to steer the wheeled robot because the accurate mathematical model doesn't exist and the uncertainties occur [10-15]. To further promote its tracking performance, the proposed AFPIDSMC scheme is applied to the wheeled robot to track the planned path simultaneously.

Now, let the desired location of the wheeled robot be a pair of two parameters (x_d, y_d) and the actual location be expressed by a pair of two parameters (x, y) which are defined in equation (4.1-2). Consider the x-axis, the tracking error and sliding surface are shown as:

$$e_x = x - x_d \tag{4.1-4}$$

$$S_x = \lambda_1 \dot{e}_x + \lambda_2 e_x + \lambda_3 \int e_x d\tau \tag{4.1-5}$$

Then the speed command of right wheel under nominal model, represented by V_{Rn}, can be represented as

$$V_{Rn} = \frac{\dot{x}_d - \lambda_1^{-1}(\lambda_2 e_x + \lambda_3 \int e_x d\tau) + \overline{\eta}\cos(\overline{\phi})\dot{\overline{\phi}}}{\overline{r}\cos(\overline{\phi})} \tag{4.1-6}$$

After applying the proposed AFPIDSMC to x-axis, the total control effort and adaptive law for right wheel is

$$V_{Rt} = V_{Rn} + \hat{c}_x (w_{1x} - w_{3x}) \tag{4.1-7}$$

$$\dot{\hat{c}}_x = \frac{\lambda_1 | w_{1x} - w_{3x} |}{\alpha} \tag{4.1-8}$$

where w_{1x}, w_{3x} are the firing strength of rule 1 and 3 in fuzzy rules base, respectively.

Then applying the AFPIDSMC to y-axis, the nominal control effort, total control effort and adaptive law for left wheel can be expressed as

$$V_{Ln} = \frac{\dot{y}_d - \lambda_1^{-1}(\lambda_2 e_y + \lambda_3 \int e_y d\tau) - \overline{\eta}\sin(\overline{\phi})\dot{\overline{\phi}}}{\overline{r}\sin(\overline{\phi})} \tag{4.1-9}$$

$$V_{Lt} = V_{Ln} + \hat{c}_y (w_{1y} - w_{3y}) \tag{4.1-10}$$

$$\dot{\hat{c}}_y = \frac{\lambda_1 | w_{1y} - w_{3y} |}{\alpha} \tag{4.1-11}$$

4.1.3. Simulation results

The simulation of the proposed system is carried out using "Matlab" package and the control parameters are given as

$$\lambda_1 = 1, \lambda_2 = 1, \lambda_3 = 2, \bar{r} = \bar{\eta} = 5cm, \alpha = 30, Z_b = -0.1, Z_a = 0.1, c = 0 \tag{4.1-12}$$

All the parameters in the proposed control systems are chosen to achieve the requirement of stability and actual specification. Four simulation cases including parameter variations and external disturbance in the kinematic equation, which appeared from the 3rd second to the 10th second, due to periodic sinusoidal commands are addressed as follows:

Case 1: without uncertainties.

Case 2: $L_x = 0.1\cos(5t)$, $L_y = 0.1\sin(5t)$

Case 3: $L_x = 0.5\cos(5t)$, $L_y = 0.5\sin(5t)$

Case 4: $L_x = \cos(5t)$, $L_y = \sin(5t)$

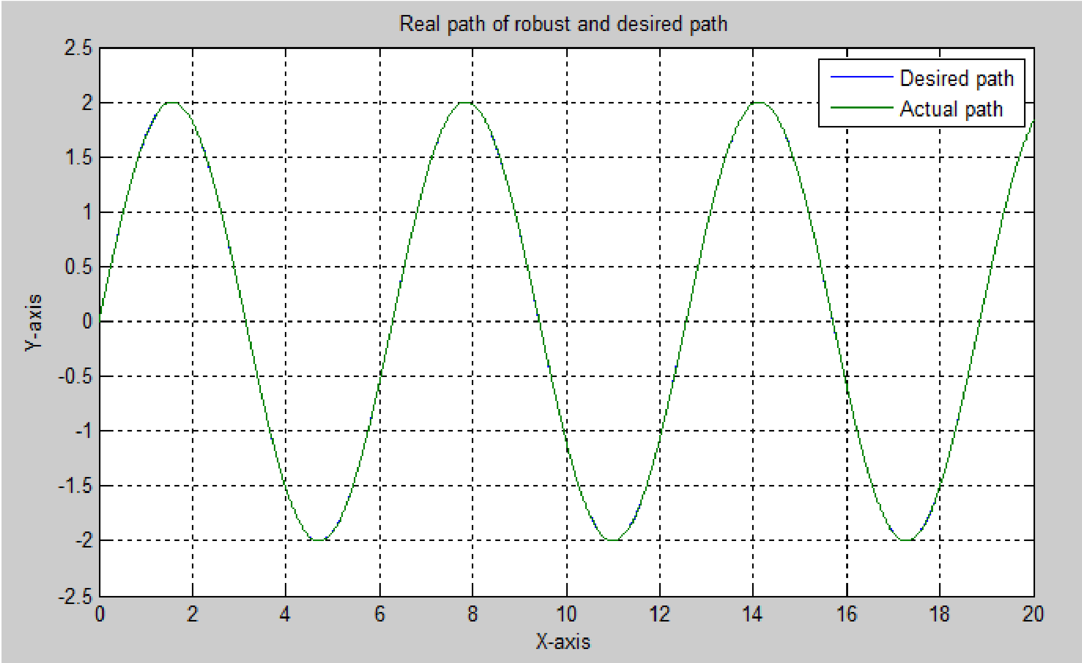

Figure 4. 3. Simulation results of conventional AFSMC at case 1

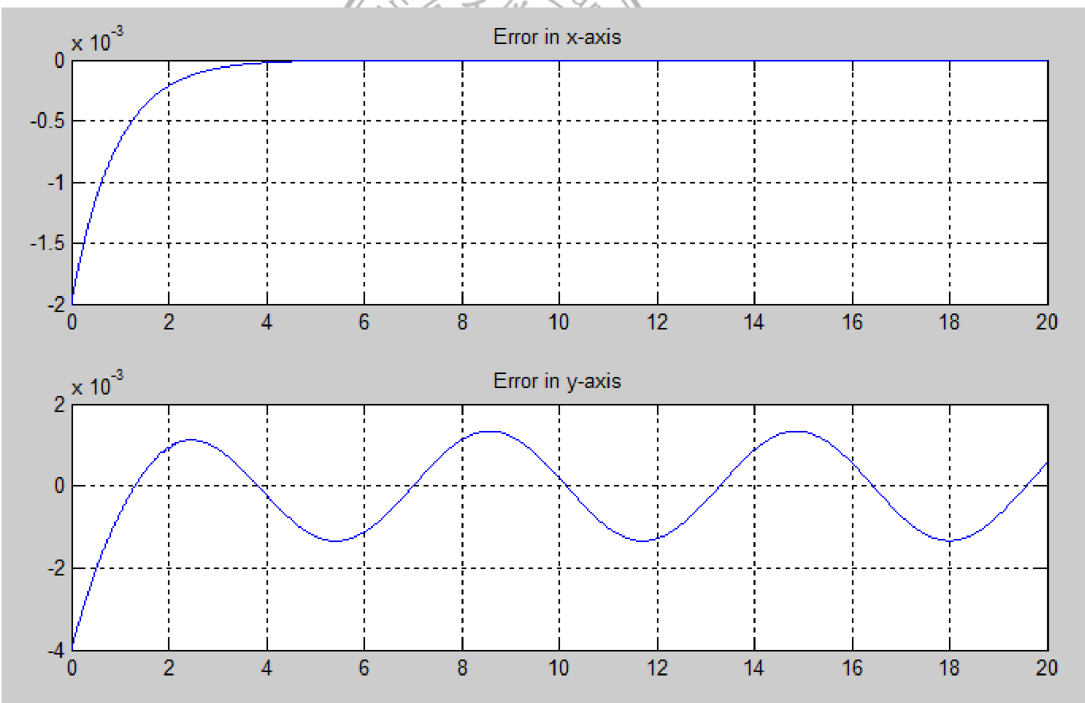

Figure 4. 4. Simulation results of conventional AFSMC at case 1

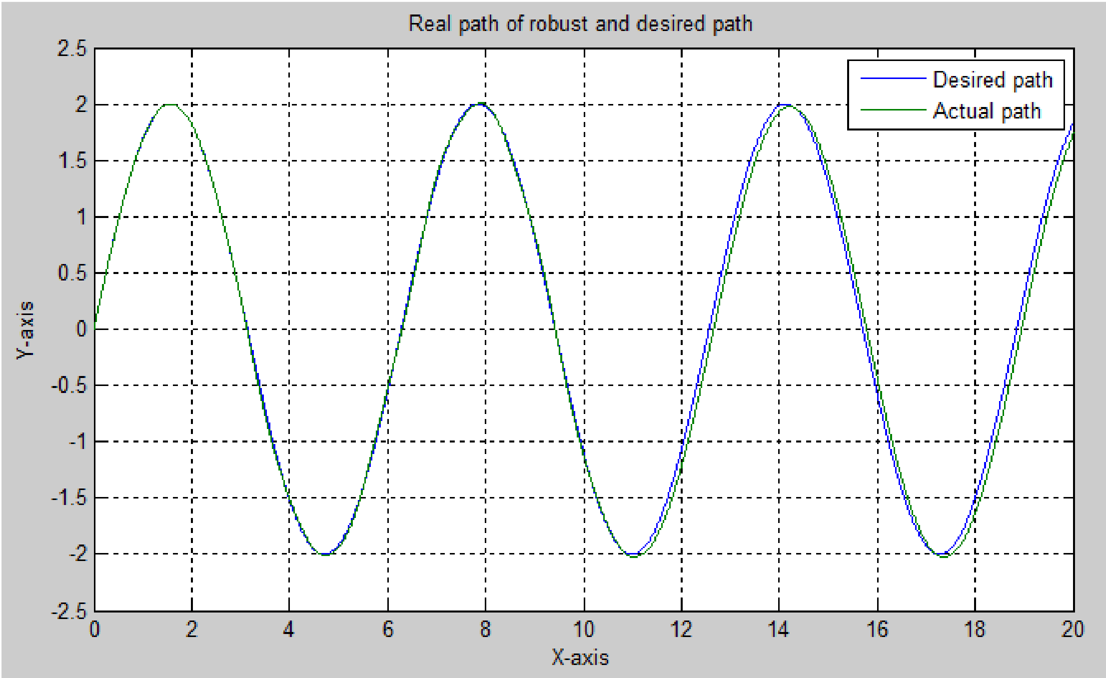

Figure 4. 5. Simulation results of conventional AFSMC at case 2

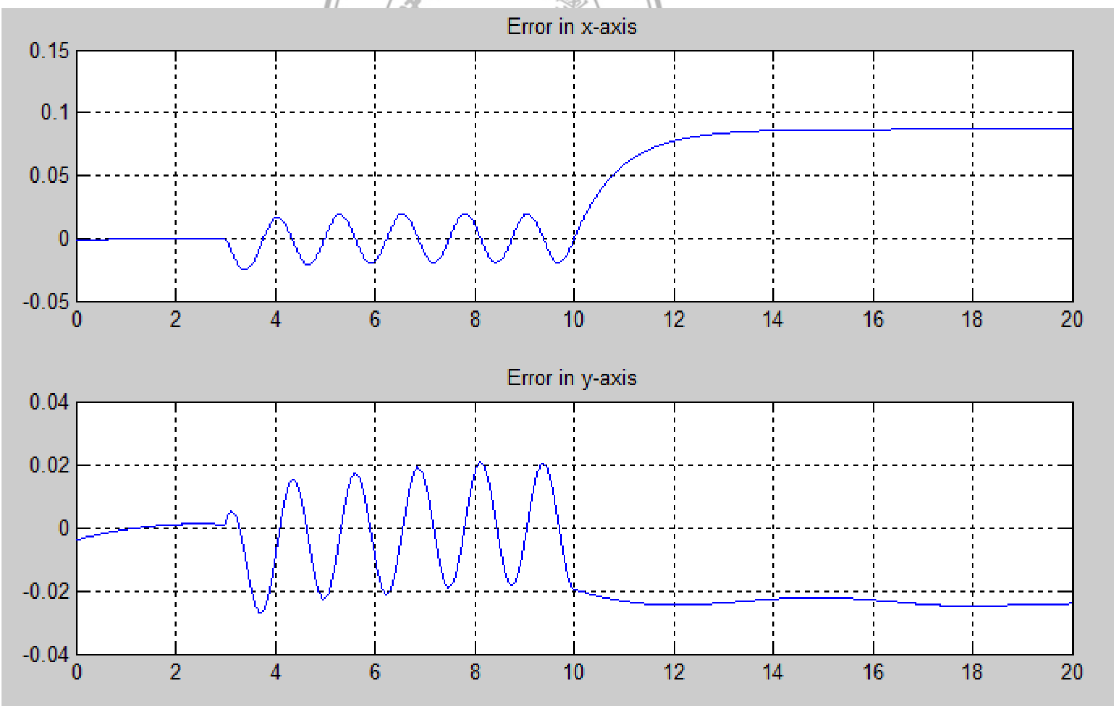

Figure 4. 6. Simulation results of conventional AFSMC at case 2

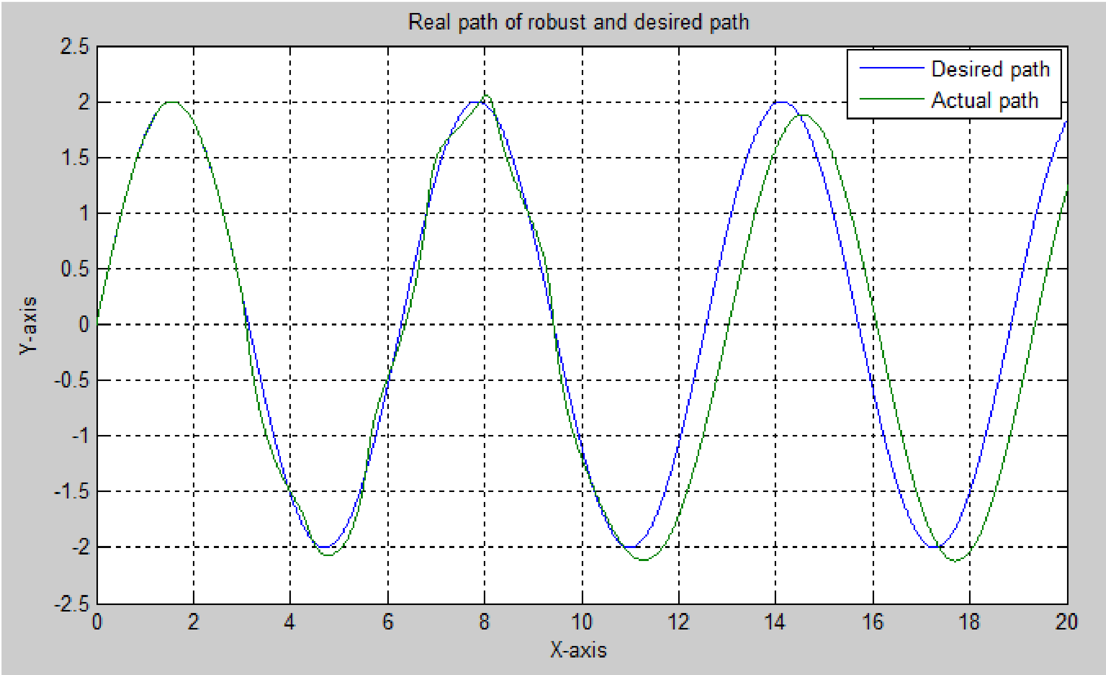

Figure 4. 7. Simulation results of conventional AFSMC at case 3

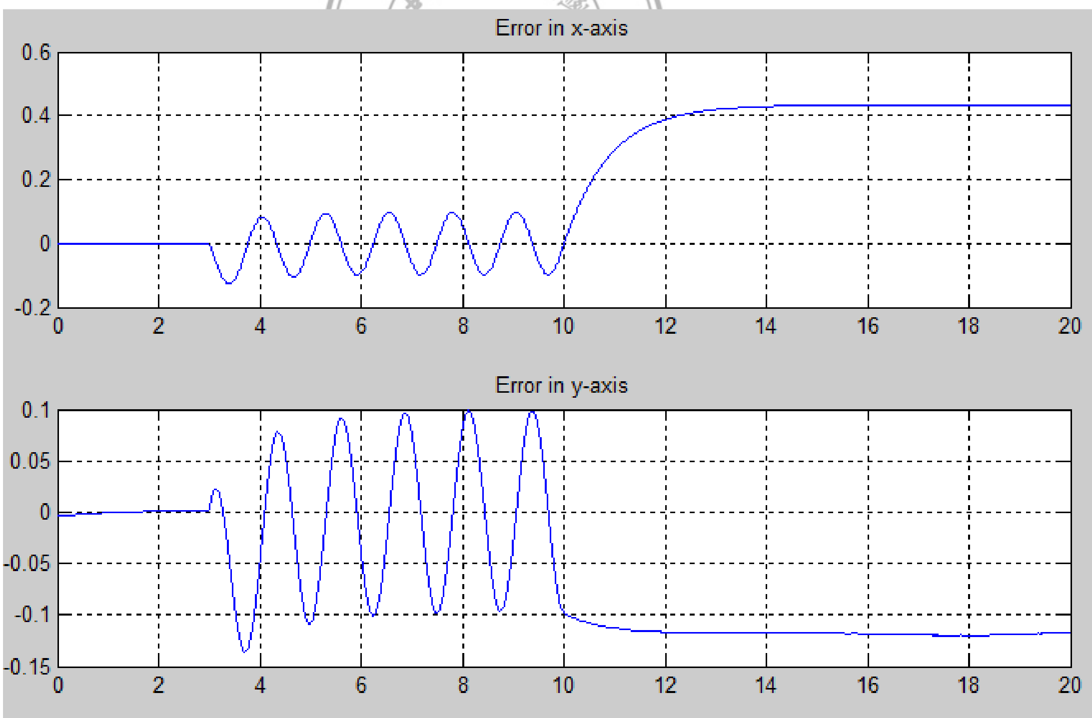

Figure 4. 8. Simulation results of conventional AFSMC at case 3

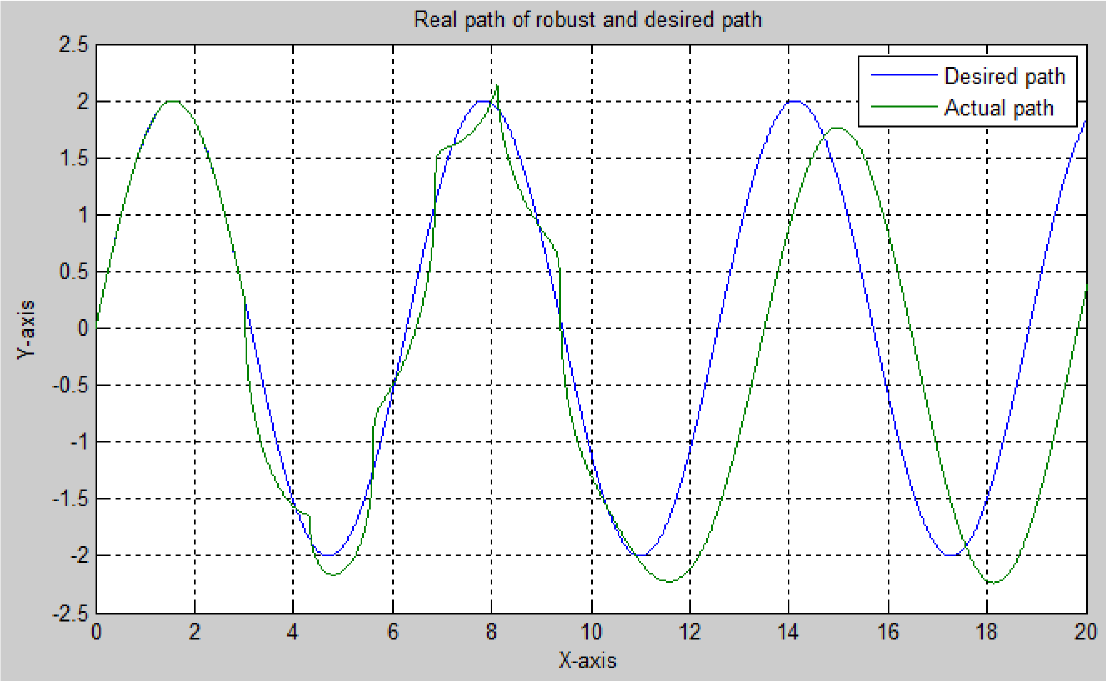

Figure 4. 9. Simulation results of conventional AFSMC at case 4

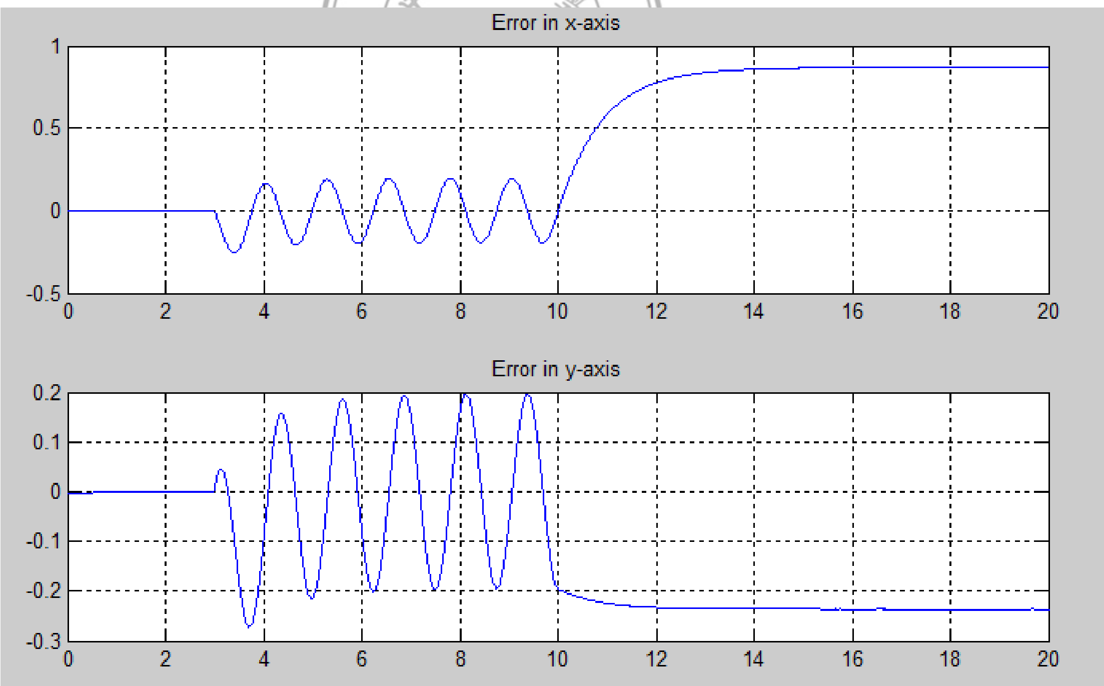

Figure 4. 10. Simulation results of conventional AFSMC at case 4

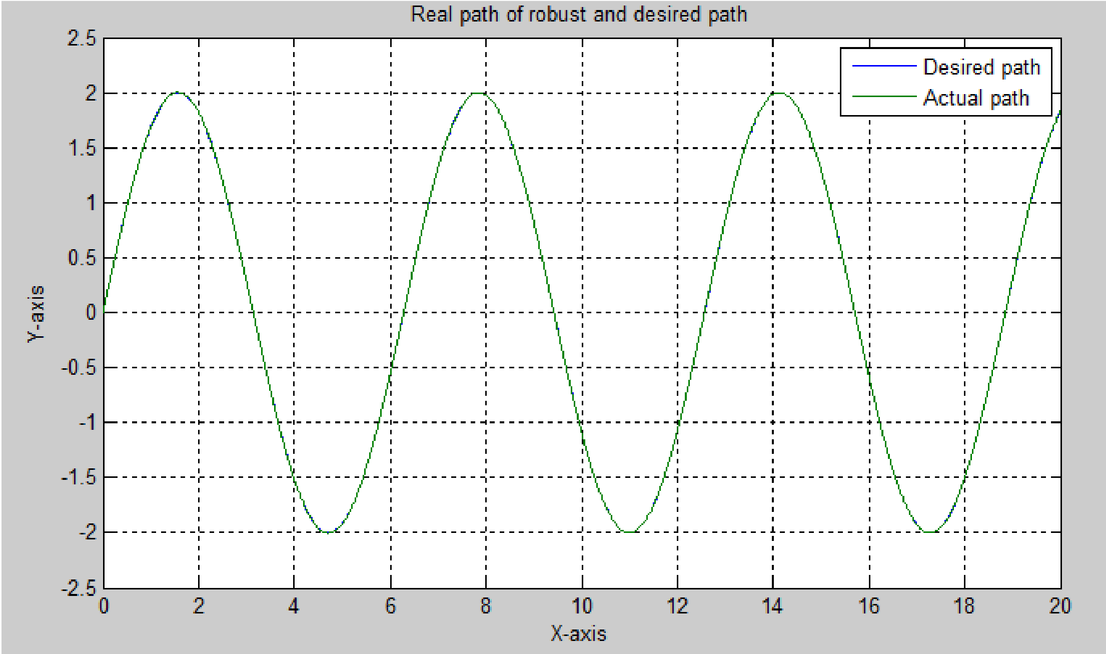

Figure 4. 11. Simulation results of proposed AFPIDSMC at case 1

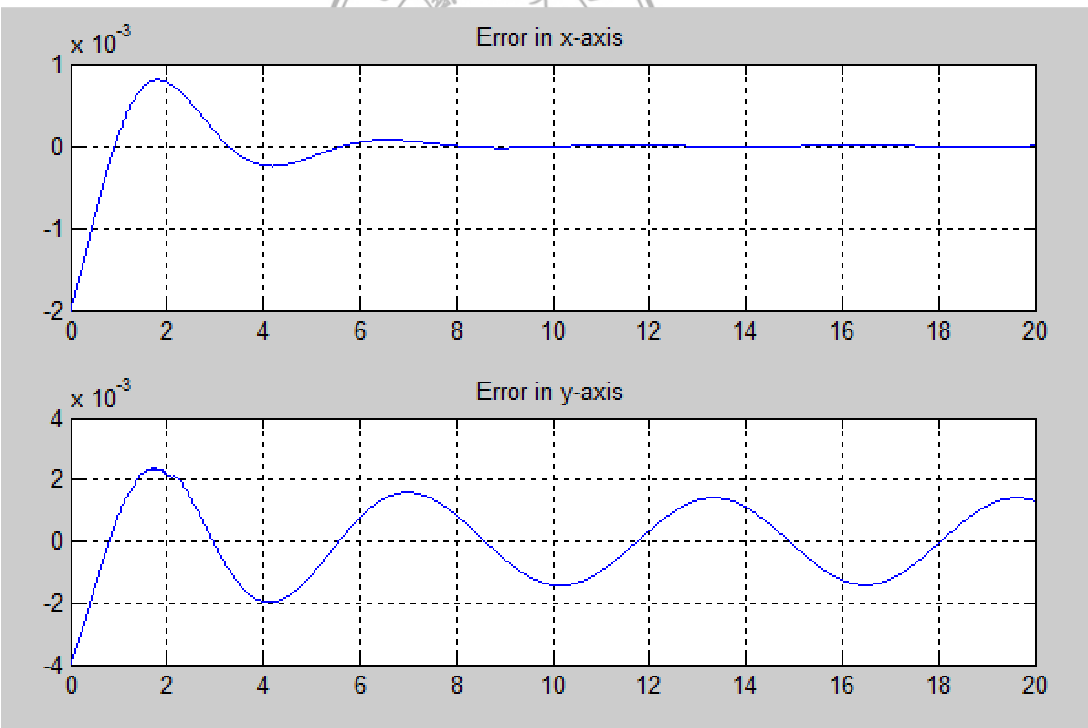

Figure 4. 12. Simulation results of proposed AFPIDSMC at case 1

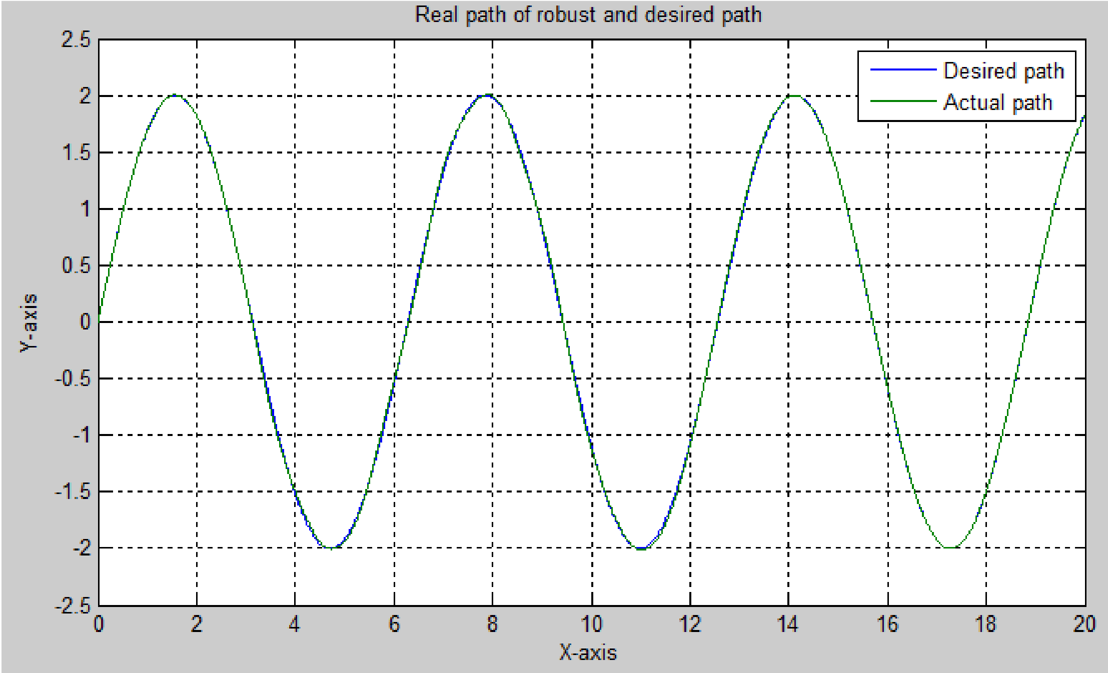

Figure 4. 13. Simulation results of proposed AFPIDSMC at case 2

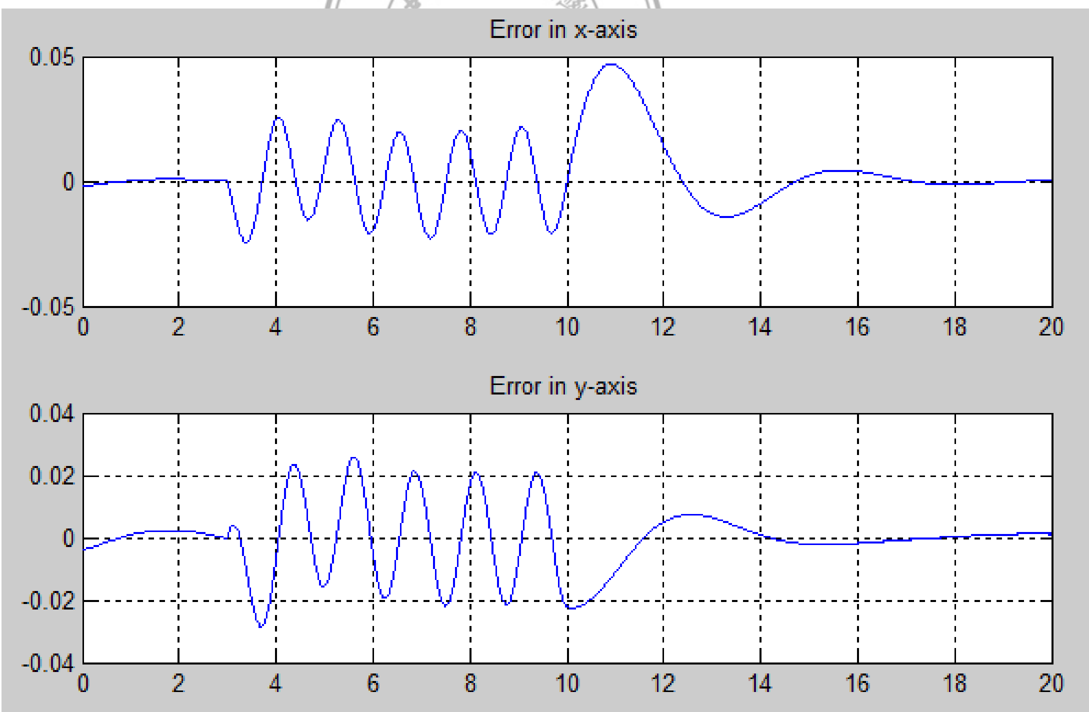

Figure 4. 14. Simulation results of proposed AFPIDSMC at case 2

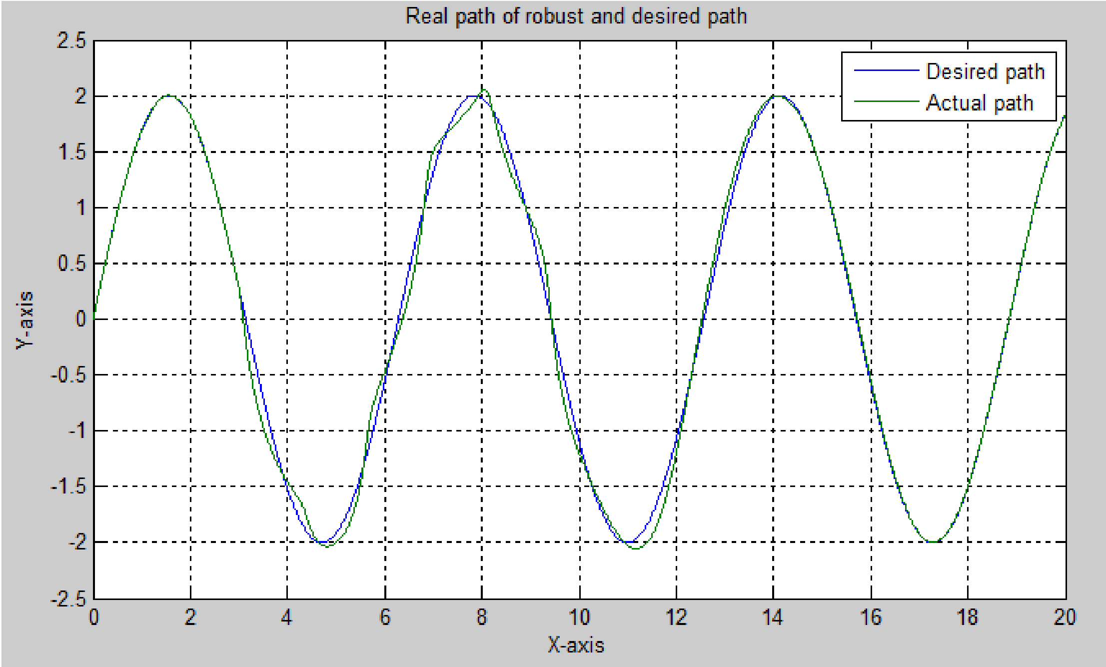

Figure 4. 15. Simulation results of proposed AFPIDSMC at case 3

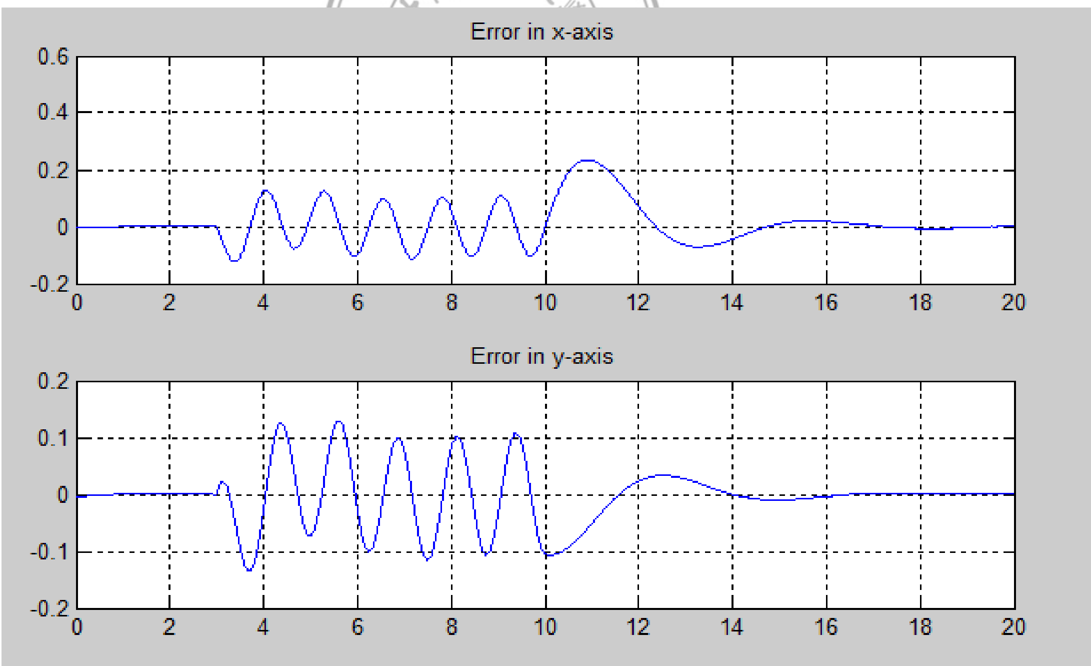

Figure 4. 16. Simulation results of proposed AFPIDSMC at case 3

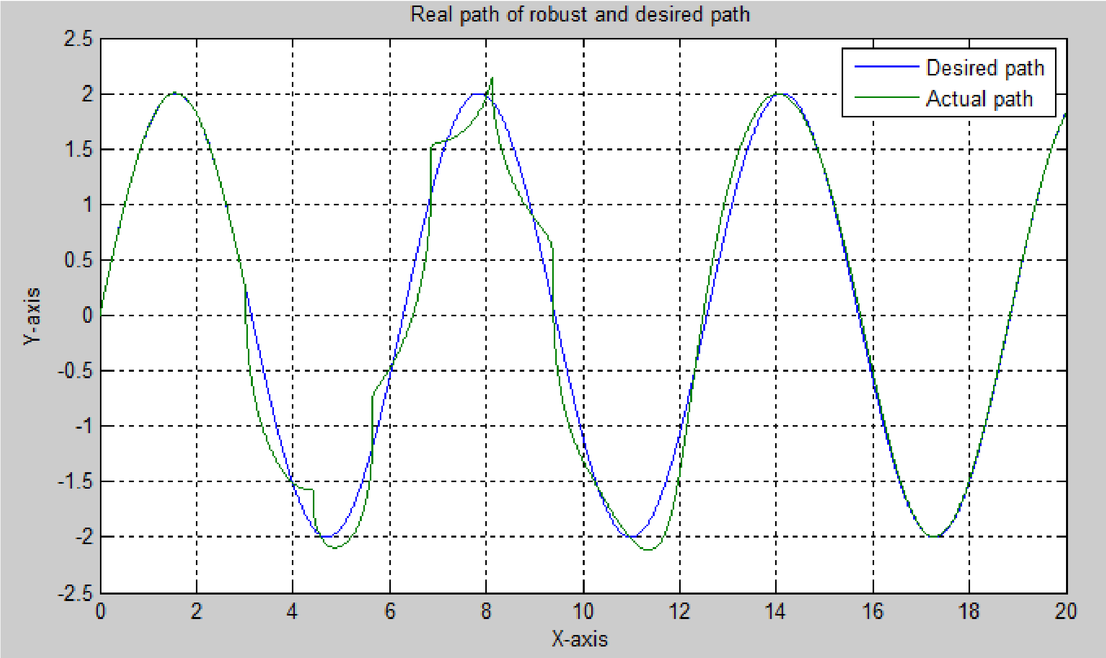

Figure 4. 17. Simulation results of proposed AFPIDSMC at case 4

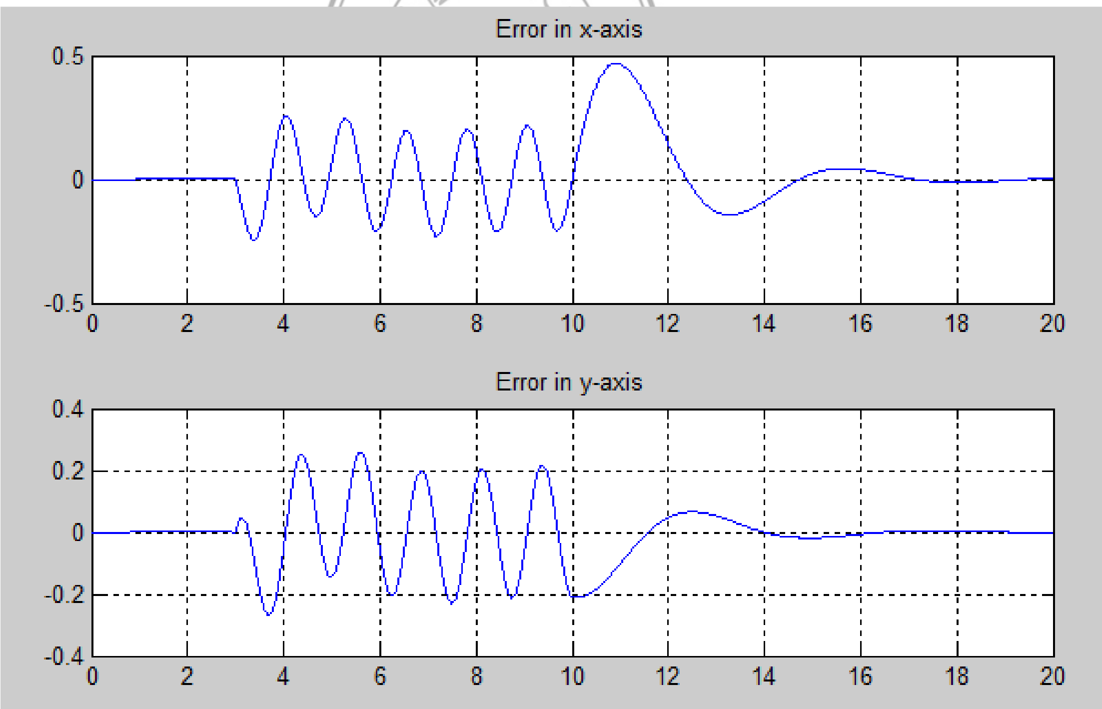

Figure 4. 18. Simulation results of proposed AFPIDSMC at case 4

Now, a conventional AFSMC tracking system [15] is considered first. The tracking responses of the AFSMC system due to periodic sinusoidal commands at Case 1, 2, 3 and 4 are depicted from Figs. 4.3 to Figs. 4.10. From the simulated results, there are no chattering phenomena, but degenerate tracking performances are resulted owing to the parameter variations and external disturbance. Finally, the proposed AFPIDSMC tracking system under rules 1, 2, 3 and the control law in equations (4.1-6, 4.1-7, 4.1-8, 4.1-9, 4.1-10 and 4.1-11) is considered. The tracking ersponses due to periodic sinusoidal command at Case 1, 2, 3 and 4 are depicted from Figs. 4.11 to Figs. 4.18.

We can see in the Figs. 4.12, 4.14, 4.16, 4.18, the steady errors in x-axis are approximately 0, 0.003, 0.01, 0.01 respectively, and the steady errors in y-axis are approximately 0.0015, 0.002, 0.001, 0.01 respectively. These values are much smaller and come closer zero value than those in AFSMC method's figures. In the Figs. 4.4, 4.6, 4.7, 4.10, the steady errors in x-axis are approximately 0, 0.087, 0.44, 0.86 respectively, and the steady errors in y-axis are approximately 0.0014, 0.025, 0.12, 0.23 respectively. Although the time responses in both of two controllers are similar which are almost 4 seconds, but the precision of the proposed AFPIDSMC is better than conventional AFSMC.

From the simulated results, not only there are no chattering phenomena but also favorable tracking response can be obtained under the occurrence of uncertainties. From the comparison by above figures, the proposed AFPIDSMC system is more suitable to track the desired path for a wheeled robot.

4.2. Balance control for a two-wheeled robot

Compared with other wheeled-robots, the two-wheeled robot has the advantages of low cost, slight volume, and small turning radius, and it is easy to carry. If the technology of balance and stability can be further improved, the performance of the two-wheeled robot would be promoted. For example, nBot, Joe, Segway, Puma, and Toyota's Winglet have been widely applied in personal transporter or data acquisition tools.

Figure 4. 19. E-NUVO wheeled robots

Figure 4. 20. Two-wheeled self balance vehicle

However, the two-wheeled robot has highly nonlinear dynamic characteristics that vary with its operating conditions. Therefore, it is difficult to evaluate the appropriate control effort to steer and balance the platform.

4.2.1. Kinematic dynamic of two-wheeled robot

The balancing diagram of a practical two-wheeled robot is shown in Figure 4.21.

Considering the balance condition, the two-wheeled robot can be approximated by a link and point mass locate at the position of the center of gravity. The dynamic equation of the inclination angles is represented as

$$\begin{aligned} \ddot{\varphi} &= f(\underline{x}) + g(\underline{x})u + d(t) \\ y &= \varphi \end{aligned} \tag{4.2-1}$$

where:

$$f(\underline{x}) = \frac{(M_c + M_w)g_a \sin(\varphi) - M_c L \sin(\varphi)\cos(\varphi)\dot{\varphi}^2}{L[\frac{4}{3}(M_c + M_w) - M_c \cos^2(\varphi)]} \tag{4.2-2}$$

$$g(\underline{x}) = \frac{\cos(\varphi)}{L[\frac{4}{3}(M_c + M_w) - M_c \cos^2(\varphi)]} \tag{4.2-3}$$

M_c is the mass of the vehicle (the mass of the two wheels is include separately)

M_w is the mass of the two wheels

g_a is the acceleration caused by gravity ($g_a = 9.8m/s^2$)

L is the half height of the robot

d(t) is the disturbance from the road

u is the control effort

φ is the inclined angle of the cant

Equation (4.2-1) shows that the balance control robot is a second-order nonlinear dynamic system, and the state vector is $\underline{x} = (\varphi, \dot{\varphi}) \in \Re^2$. The control problem is to steer the state to track a desired state vector $\underline{x}_d = (\varphi_d, \dot{\varphi}_d) \in \Re^2$. The tracking error is defined as $\underline{e} = (e, \dot{e})^T$ where $e = x - x_d$ and $\dot{e} = \dot{x} - \dot{x}_d$.

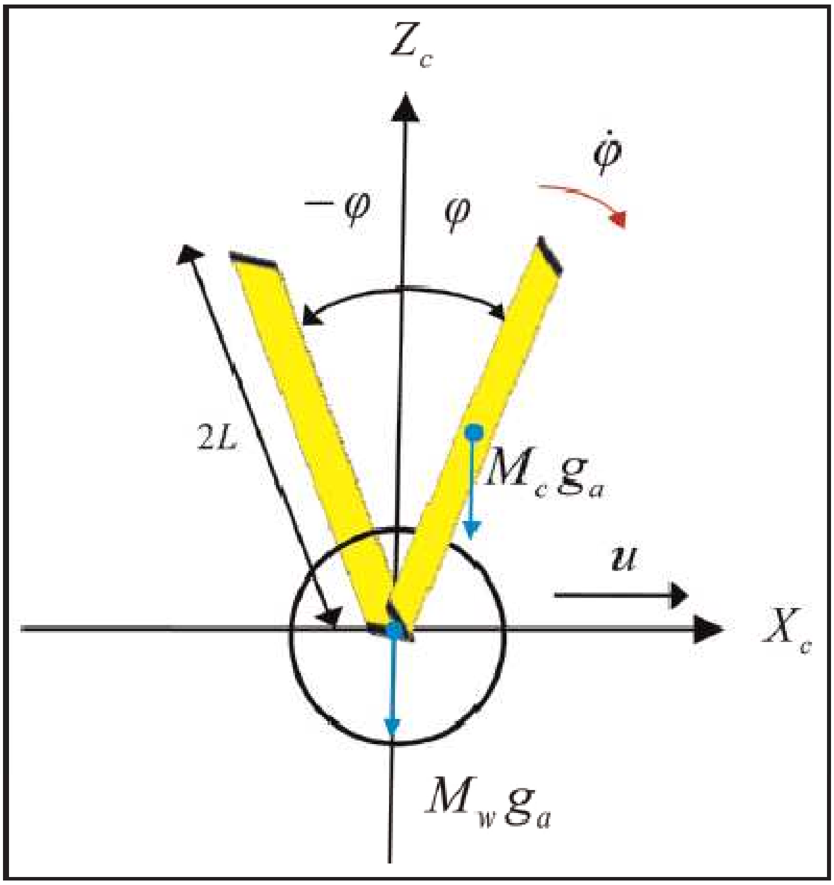

Figure 4. 21. Balancing diagram of a two wheeled robot

4.2.2. Design of AFPIDSMC

The sliding surface is chosen as equation (2.2-2) and can be rewrite as below:

$$S = \lambda_1 \ddot{e} + \lambda_2 \dot{e} + \lambda_3 e + \lambda_4 \int e d\tau \tag{4.2-4}$$

In which λ_1, λ_2, λ_3, λ_4 is a positive real number. $f(\underline{x})$ and $g(\underline{x})$ are estimated by equation (4.2-2) and (4.2-3), respectively. The control effort under nominal model, represented by u_0 can be represented as

$$u_0 = \frac{1}{g(\underline{x})}[\ddot{\varphi}_d - f(\underline{x}) - K] \tag{4.2-5}$$

where: $$K = \lambda_2 \dot{e} + \lambda_3 e + \lambda_4 \int e d\tau \tag{4.2-6}$$

with consideration $\lambda_1 = 1$.

The total control effort and the adaptive tuner are presented by the equation (3.3-1) and equation (3.3-4), respectively.

4.2.3. Simulation results

The simulations were conducted using a MATLAB package. The control objective is to push the inclined angle φ of the two-wheeled robot to track the desired trajectory $\varphi_d = 0^{o}$, $\dot{\varphi}$ to track the desired trajectory $\dot{\varphi}_d = 0^{o}/s$ and $\underline{e}$ converges to 0. The specifications of the platform were as follows: $M_w = 1$kg, $M_c = 0.1$kg, $L = 0.5$ m, $g_a = 9.8 m/s^2$ and the sampling interval of the balance control loop was set to $2ms$ in the simulations. The control parameters were chosen as equation (4.2-4) where

$$\lambda_1 = 1,\ \lambda_2 = 18,\ \lambda_3 = 10,\ \lambda_4 = 0.1,\ \alpha = 3,\ c = 0$$

The initial system state was $x(0) = (10^{o}, 2.86^{o}/s)^T$; and the time interval was $0 \le t \le 30s$.

For comparison, a conventional AFSMC was considered. Simulation cases, including four different disturbances, were addressed as follow.

Case 1: No disturbance $d(t) = 0$

Case 2: $d(t) = 0.5$ occurring at 10^{th} second and removing at 11^{th} second.

Case 3: $d(t) = 0.5$ constant external disturbance from 10^{th} second to 20^{th} second.

Case 4: $d(t) = 0.5\cos(t)$ external disturbance from 10^{th} second to 20^{th} second.

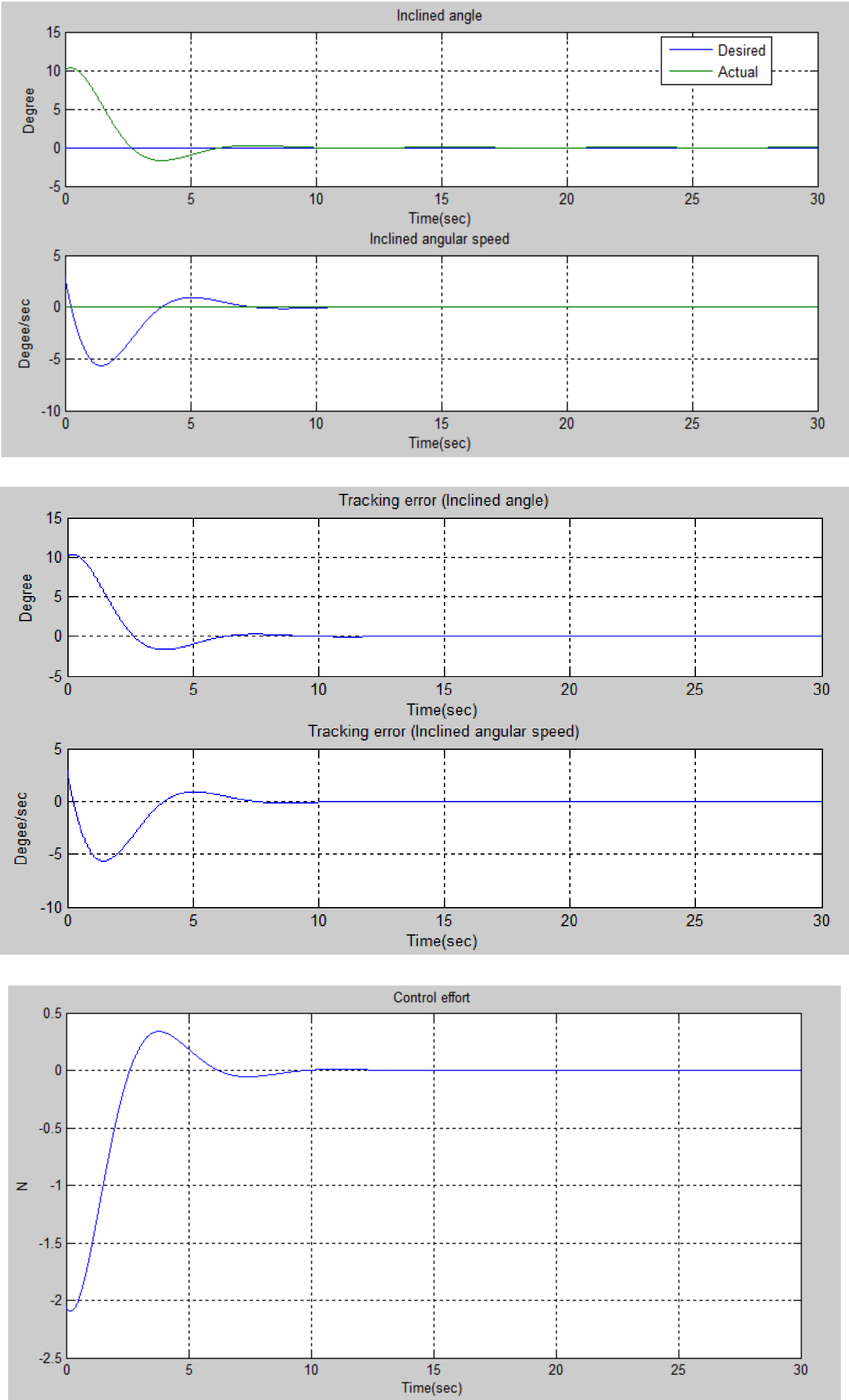

Figure 4. 22. Simulation results of conventional AFSMC at case 1

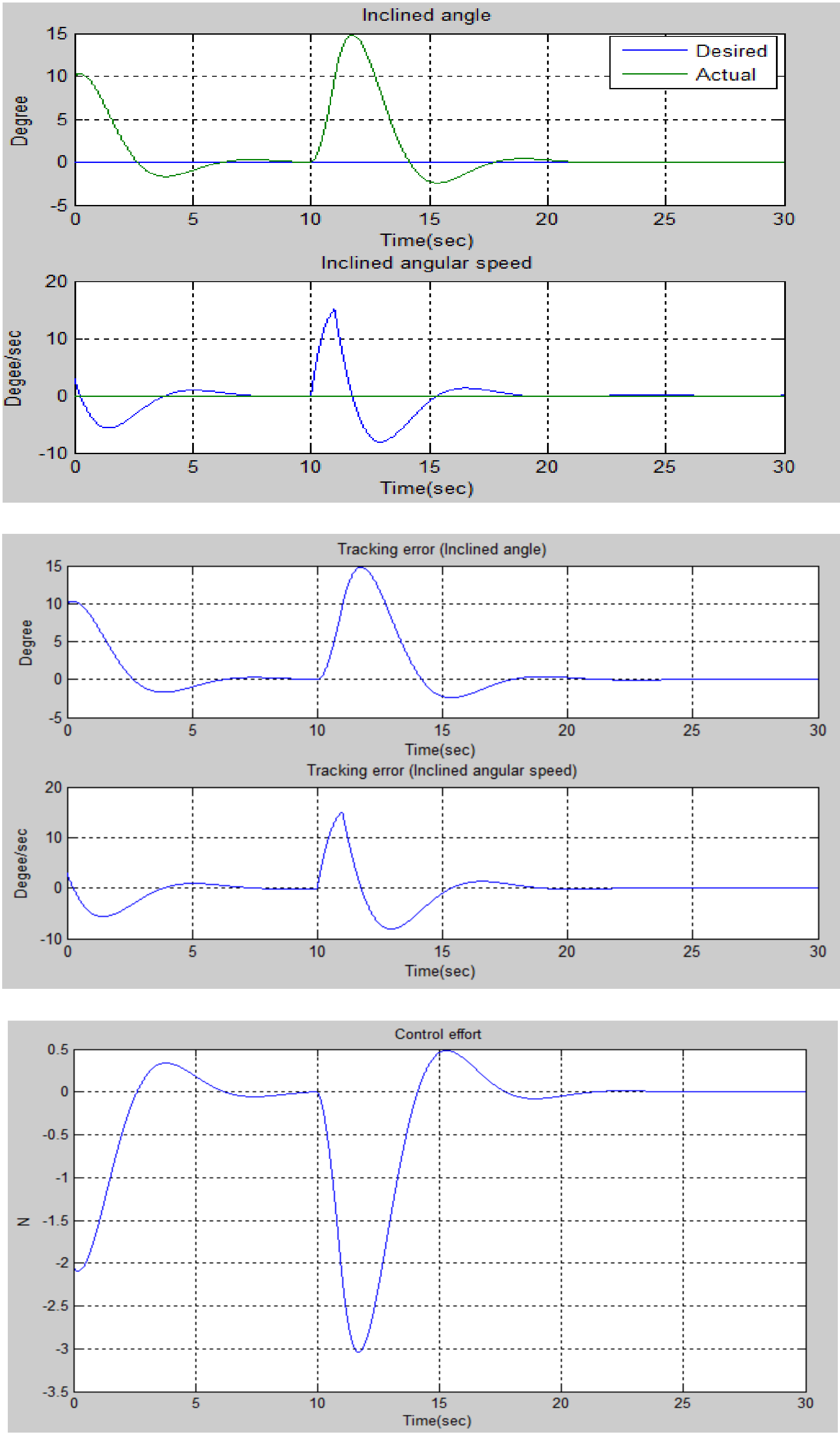

Figure 4. 23. Simulation results of conventional AFSMC at case 2

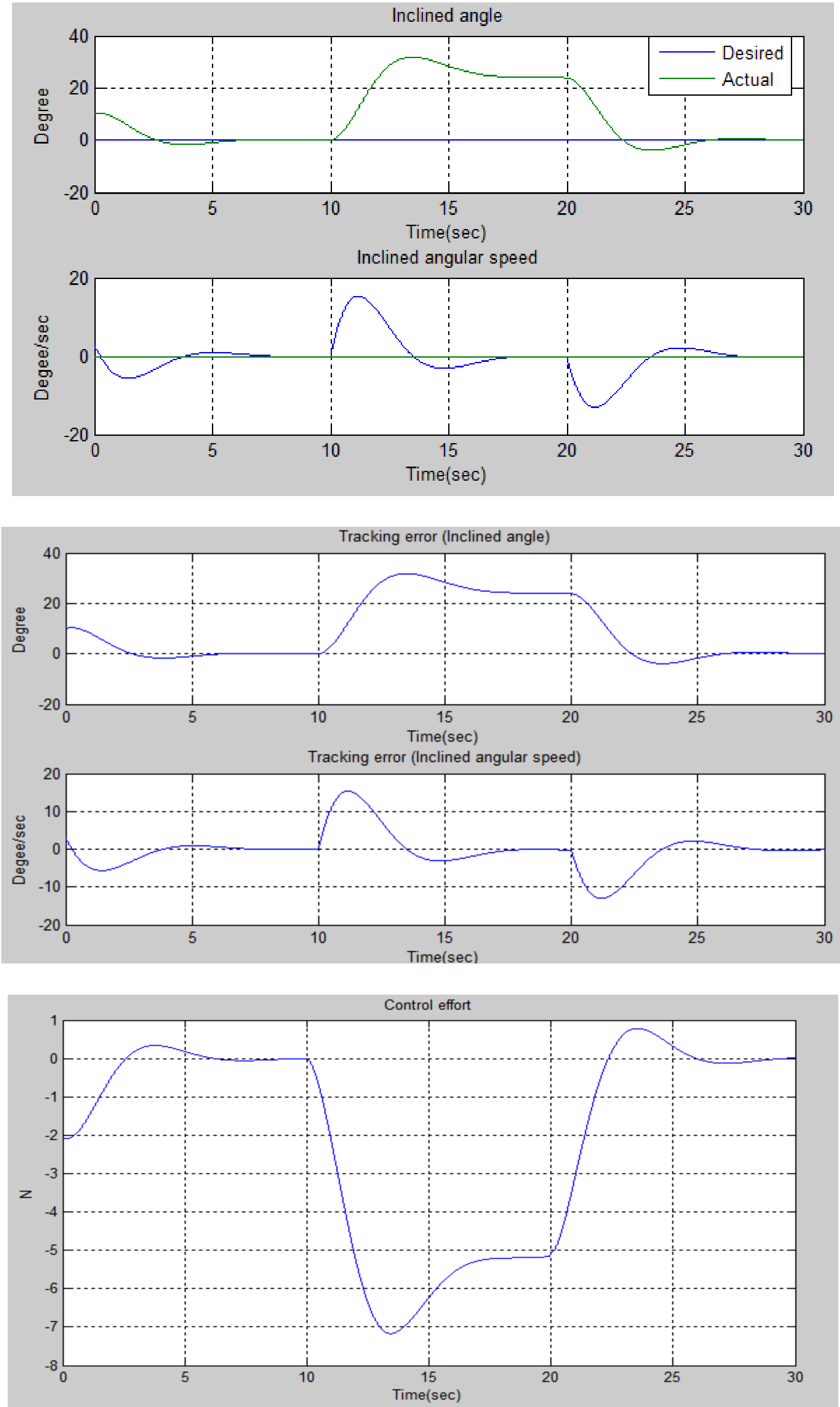

Figure 4. 24. Simulation results of conventional AFSMC at case 3

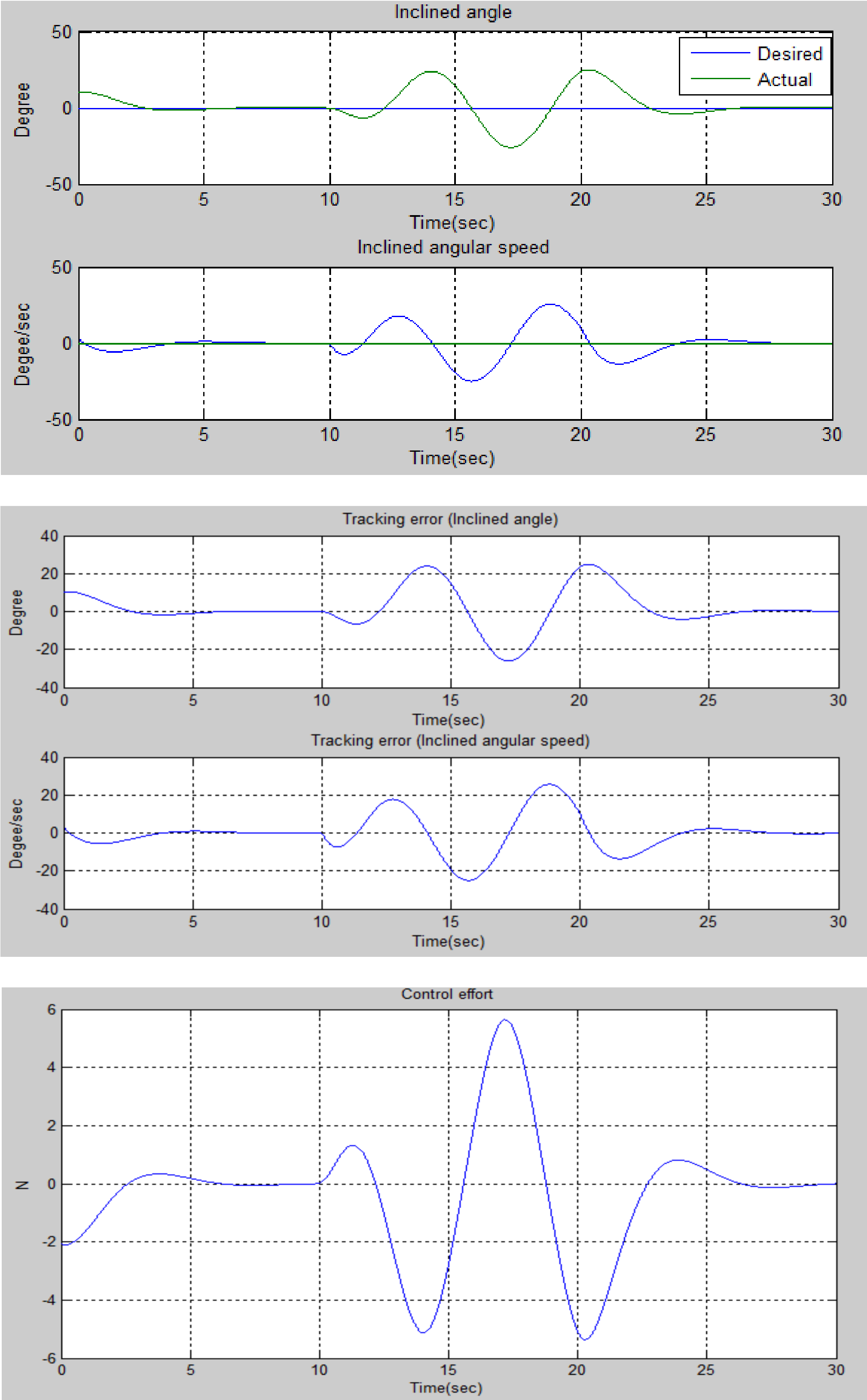

Figure 4. 25. Simulation results of conventional AFSMC at case 4

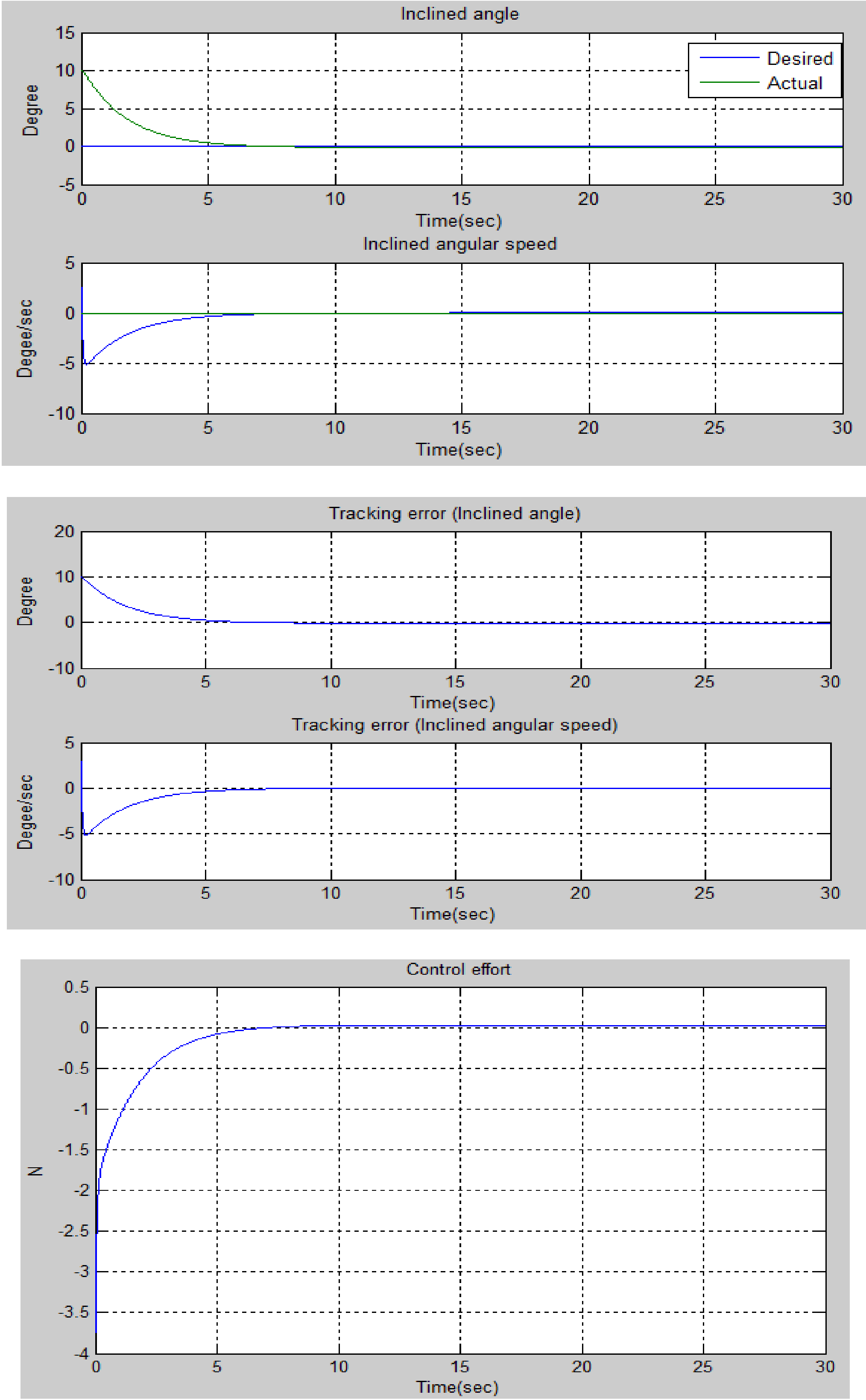

Figure 4. 26. Simulation results of proposed AFPIDSMC at case 1

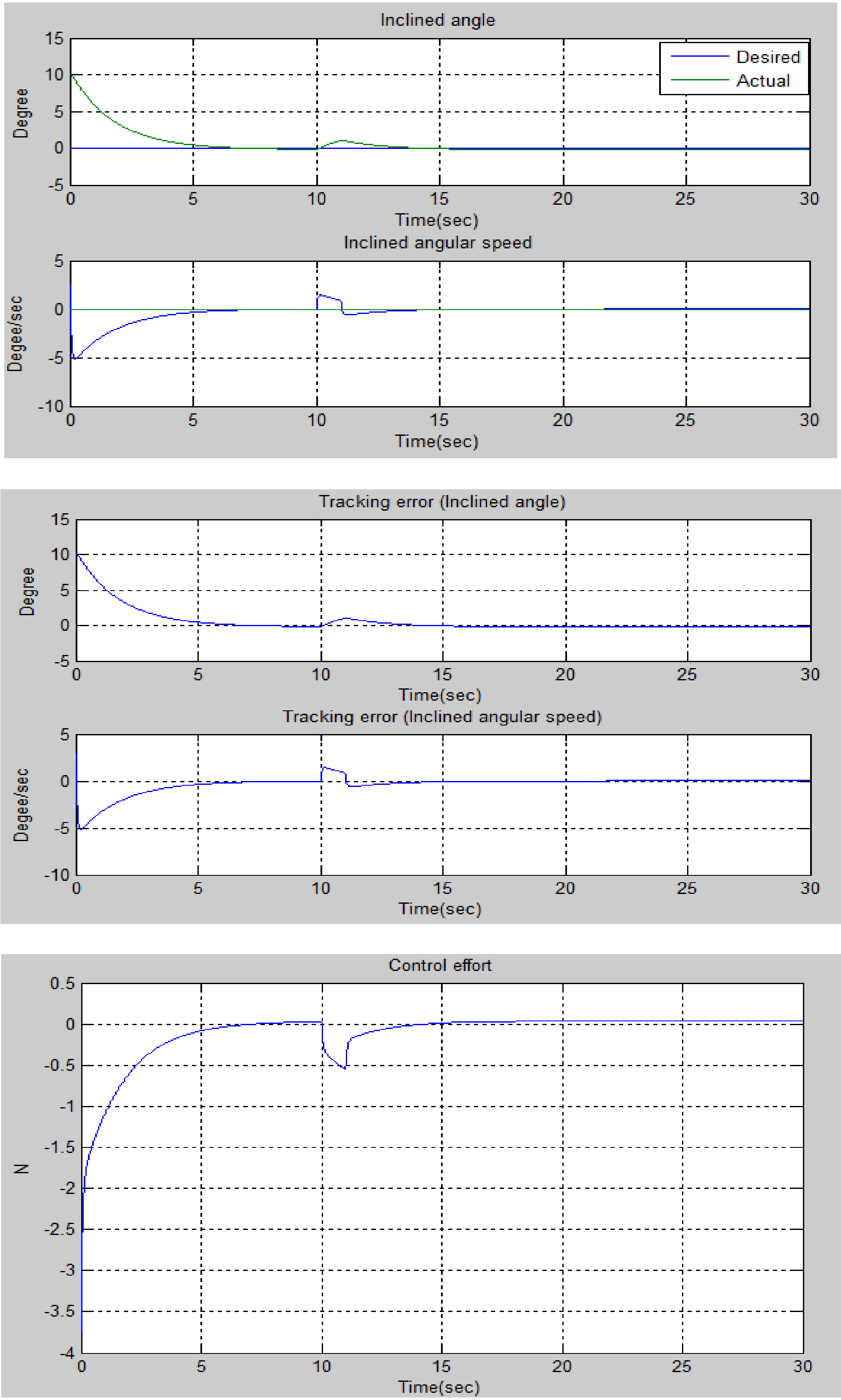

Figure 4. 27. Simulation results of proposed AFPIDSMC at case 2

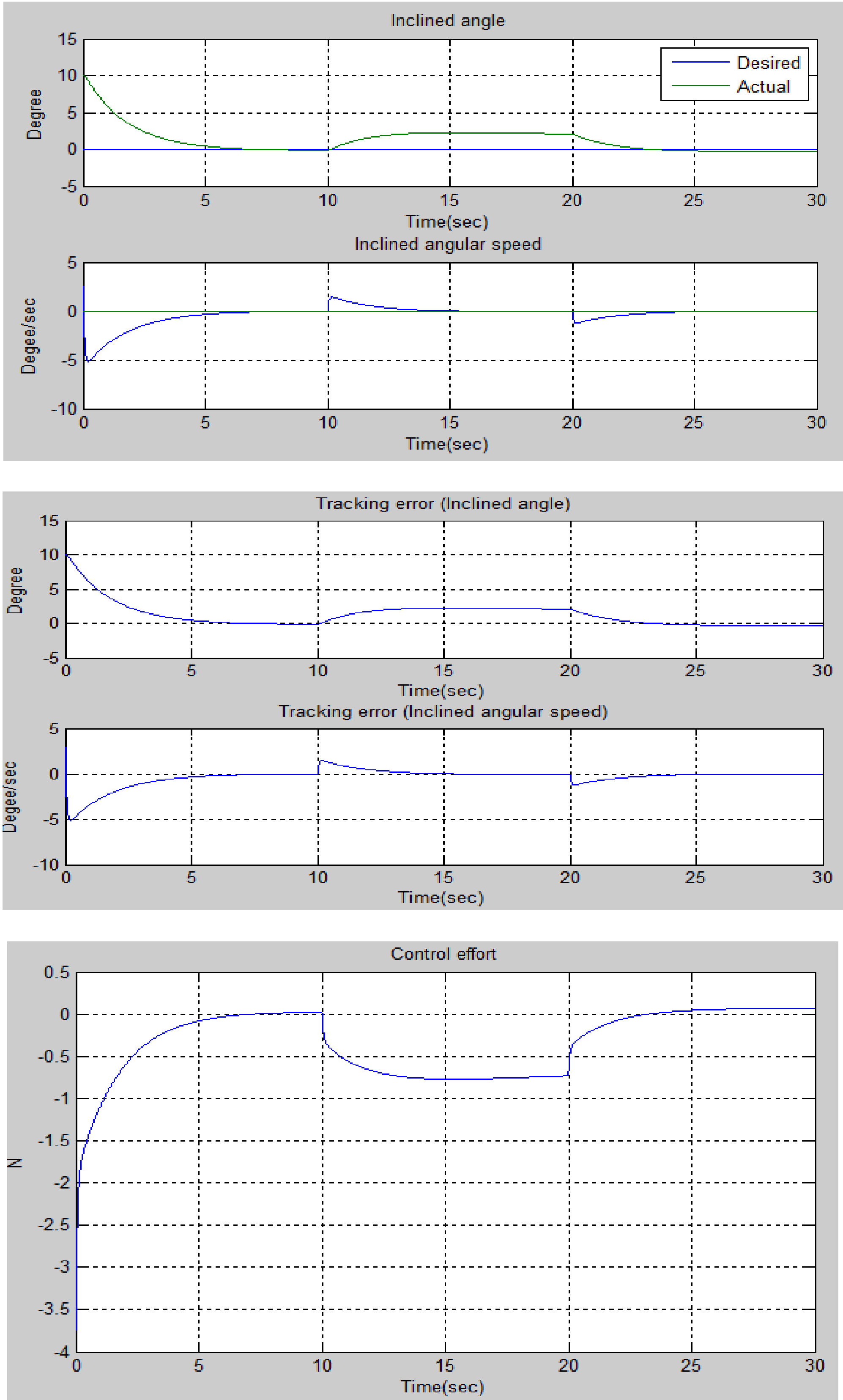

Figure 4. 28. Simulation results of proposed AFPIDSMC at case 3

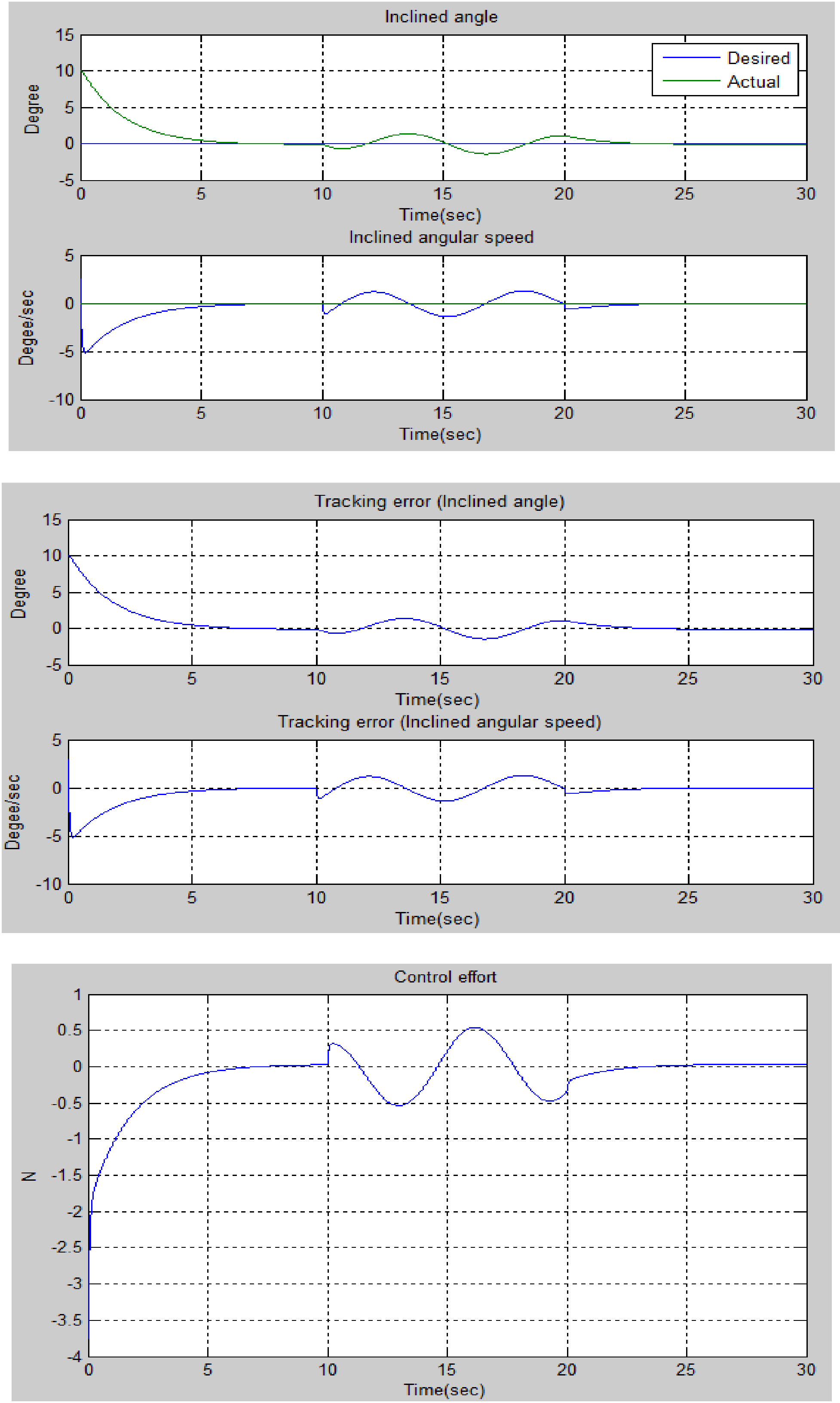

Figure 4. 29. Simulation results of proposed AFPIDSMC at case 4

Now, a conventional AFSMC was considered first. From Fig. 4.22 to Fig. 4.26, we can see that the time response of system is approximately 7 seconds to get the stable state from the initial state. The control effort during this period is nearly 2.1 N. If there is no disturbance, the performance of system is shown in Fig. 4.22. When the disturbance appears, the dynamic error will be increased, but the performance are depended on the type of disturbance and the time they affect to system. In Fig. 4.21, disturbance appeared from 10^{th} second to 11^{th} second, the maximum inclined angle and the inclined angular speed are 15^{o} and 15^{0}/s, respectively. Still same that constant disturbance, but if the affected time is longer such as in case 3, the maximum inclined angle and the inclined angular speed are increased to 36^{o} and 15^{0}/s, respectively. In case 4, when we changed the disturbance, the maximum inclined angle and the inclined angular speed are increased to 25^{o} and 25^{0}/s, respectively. However, the system still be stable after that. The maximum control effort of system in case 1, 2, 3 and 4 are 2.1, 3, 7 and 5.6 N, respectively.

When we used the AFPIDSMC, the performance of system in case 1 is almost similar with the performance in Fig. 4.22. However, when the disturbance appears, there are some differences in Fig. 4.27, 4.28 and 4.29. The maximum inclined angle in case 2, 3, and 4 are 1^{o}, 2.5^{o} and 2^{o}, respectively; and the maximum inclined angular speed in case 2, 3, 4 are 2, 2.2, and 2^{o}/s. They are smaller than the ones we get from AFSMC in Fig. 4.23, 4.24 and 4.25. Similarly, the maximum control efforts are 0.5, 0.7 and 0.5 N. Thus, the performance of AFPIDSMC is better than a conventional AFSMC.

4.2.4. Experimental results

In Section 4.2.3, we discussed about the simulation results. Base from those results, we can confirm that AFPIDSMC method has better performance than a conventional AFSMC. However, because the real environment is always different with the simulation environment, thus we need to do some experimental test. The experimental results are provided by using Two Wheel robot e-nuvo.

a) About the platform

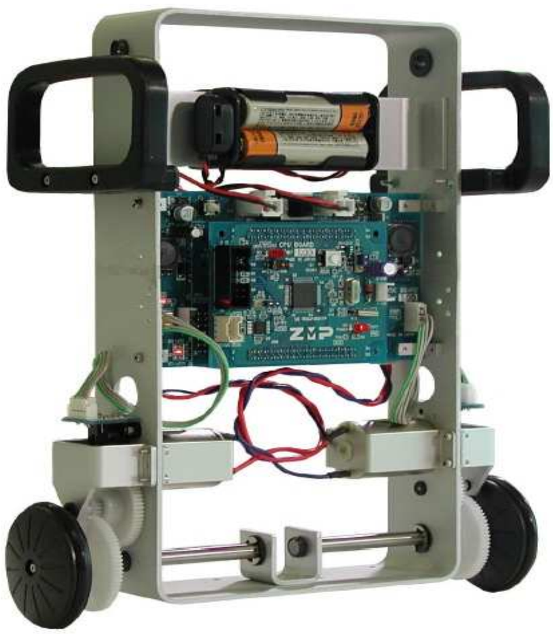

Figure 4. 30. Two wheeled robot E-NUVO

The specification of this platform is shown in Table 4.1, as well as the hardware construction and control system are shown in Figure 4.31 and 4.32, respectively.

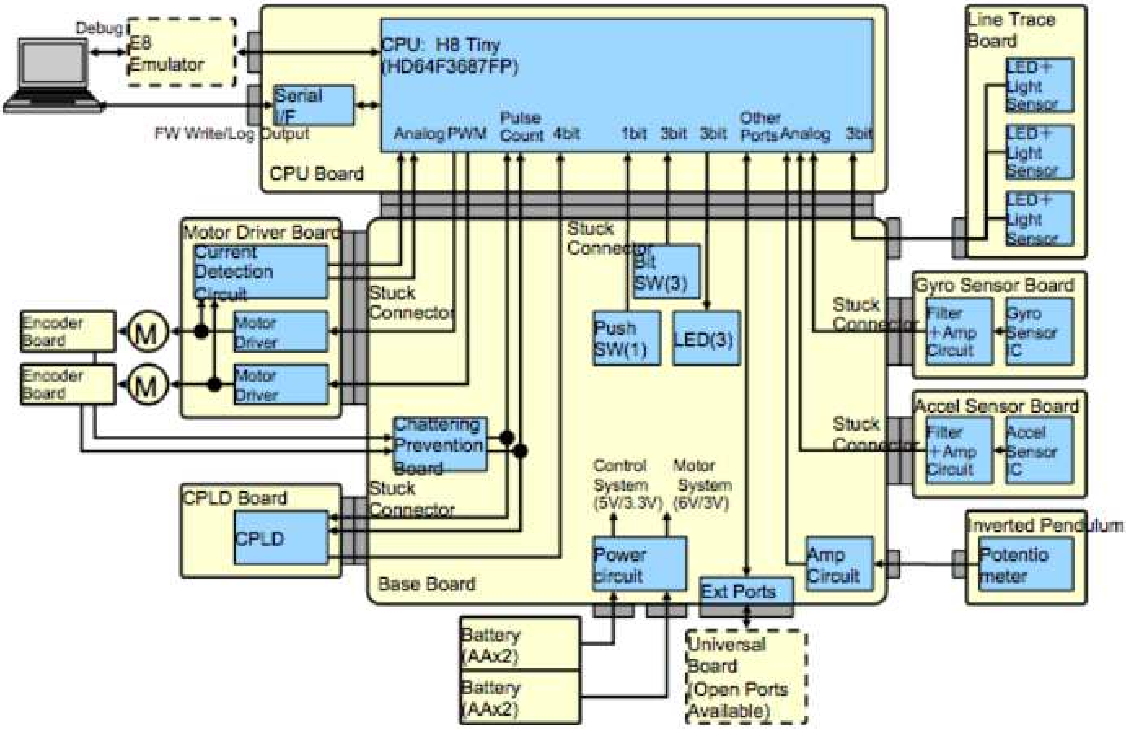

Figure 4. 31. Hardware construction of two wheeled robot E-NUVO

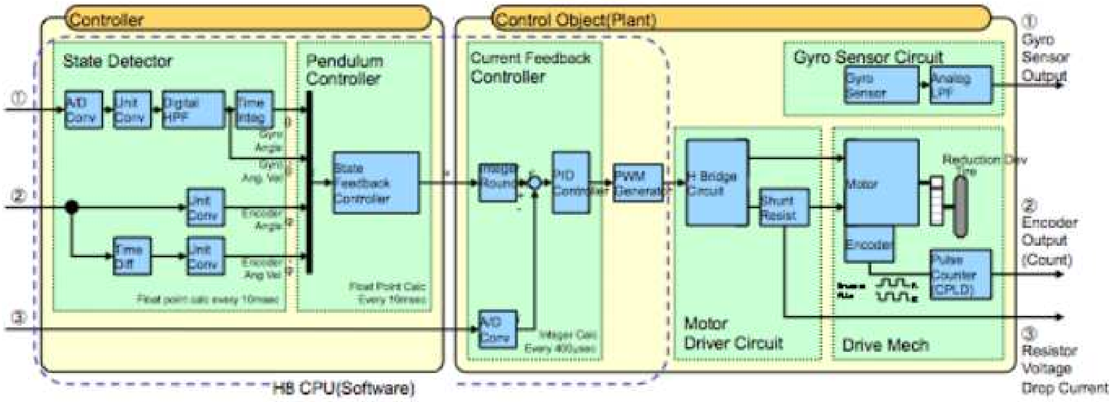

Figure 4. 32. Control system of two wheeled robot E-NUVO (inverted pendulum/one motor case)

Product Name		Wheeled Robot e-nuvo WHEEL ver.1.1
CPU		ZMP Original Generic CPU Board(x1) - Renesas Technology H8 Tiny (HD64F3687FP)
CPLD (For Encoder Pulse signal Processing)		ZMP Original Generic CPLD Board(x1) - Altera MAX II EPM240T100C5
Actuator		Mabuchi DC Motor RE-280RA, Reduction Gears 30
Motor Driver		ZMP Original 2ch Motor Driver Board(x1) - H Bridge Circuitx2 - High Precision Elec. Feedback Circuitx2
Sensors	Angle Sensor	ZMP Original Encoder Board(x2) - Rotary Encoder: Kodenshi KE203(Resolution 100[pulse/rev]) - Output resol: 0.03[deg](=360deg/100/4 rotary/deceleration ratio 30)
	Pose Sensor	ZMP Original Gyro Sensor Board(x1) - Gyro Sensor: Murata ENC-03RCx1
	Accel Sensor	ZMP Original Accel Sensor(x1) - Accel Sensor: ANALOG DEVICES ADXL322JCP
	Pendulum Angle Sensor	Murata Potentiometer
	Line Trace Sensor	ZMP Original Line Tracing Sensor Board(x1)(3ch Photosensor)
PC I/F		Control CPU5[v], CPLD3.3[v] (1.2[v]Batt x2, boosted) Motor 3[v]/6[v](variable) (1.2[v]Batt x2, boosted)
Recommended Development Environment	Integrated Development	Renesas Electronics HEW(High-performance Embedded Workshop)
	Flash Writing Tool	Renesas Electronics FDT(Flash Development Toolkit)

Table 4. 1. Specification of two wheel robot E-NUVO

b) Experimental Processing

The embedded microcontroller (HD64F3687FP) included analog-to-digital (A/D) converters, a time integrator, digital-to-analog (D/A) converters, a digital high-pass filter (HPF), timers, input–output (parallel I/O), data memory, and program memory. Other driving and actuating components included a pulse-width modulation (PWM) generator, a Gyro sensor (Murata ENC-03RC), an H Bridge circuit, a driving motor (RE- 280RA), a power supply, and a mechanical chassis. The AFPIDSMC is responsible for calculating the necessary control effort according to the detected inclined angle and inclined angular speed of the cant. The specification parameters of the platform were as follows: M_c = 686g, M = 60.5g, L=14.8 cm, and g_a = 9.8 m/s^2. The initial inclined angle was $\varphi(0) \cong 0^o$. The experimental results are provided in two case:

Case 1: No disturbance.

Case 2: Have disturbance.

The experimental results of the proposed AFPIDSMC are shown in Figure. 4.35 and 4.36. In additional, the tracking responses with a conventional AFSMC are shown in Figure 4.33 and 4.34 to compare with proposed method.

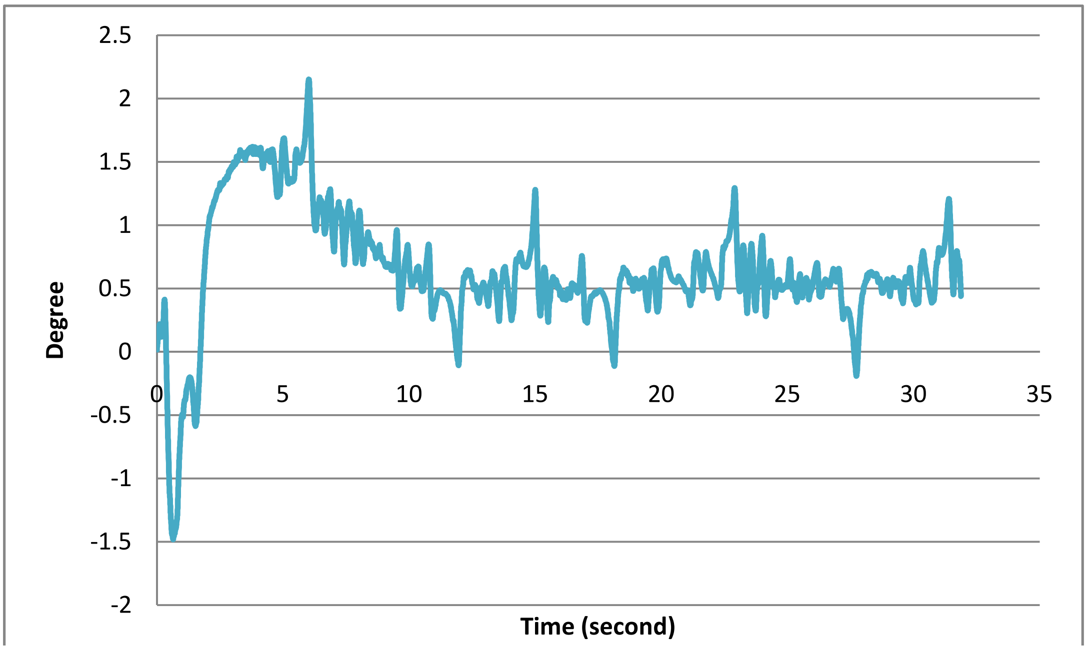

(a)

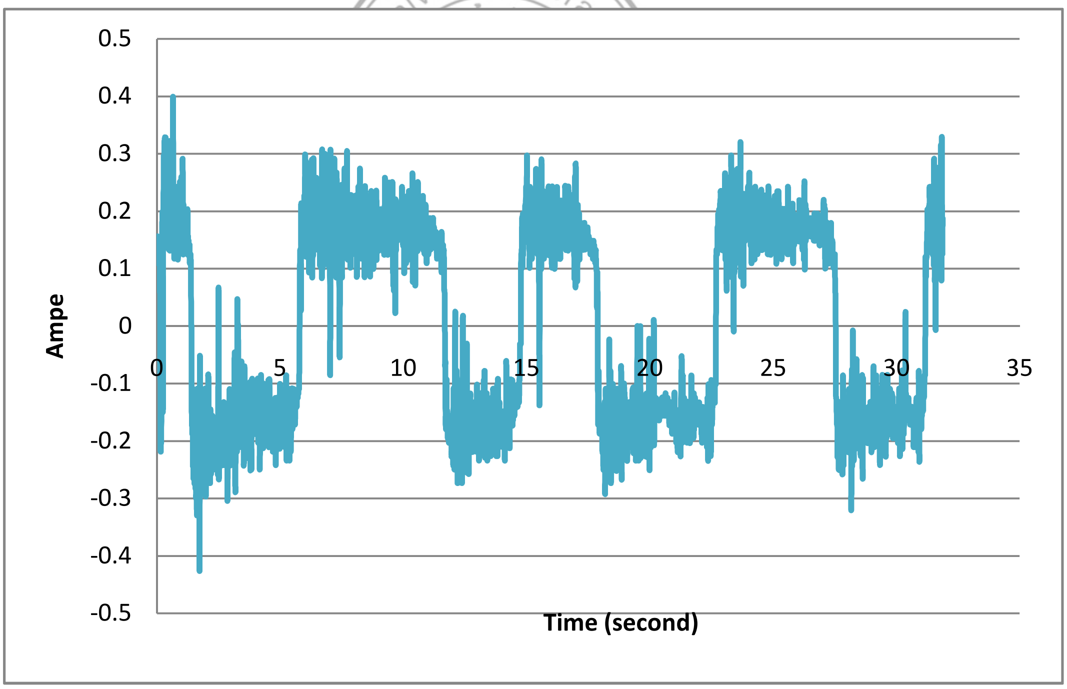

(b)

Figure 4. 33. Experimental results of conventional AFSMC at case 1

(a) Inclined angle, (b) Output current of PWR for one wheel

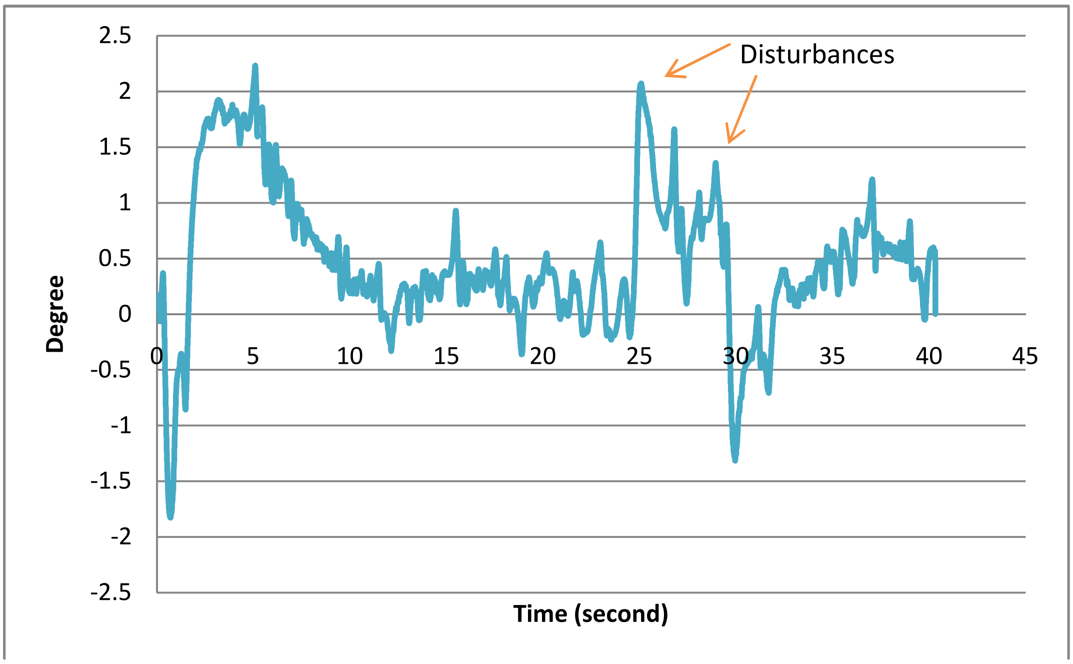

(a)

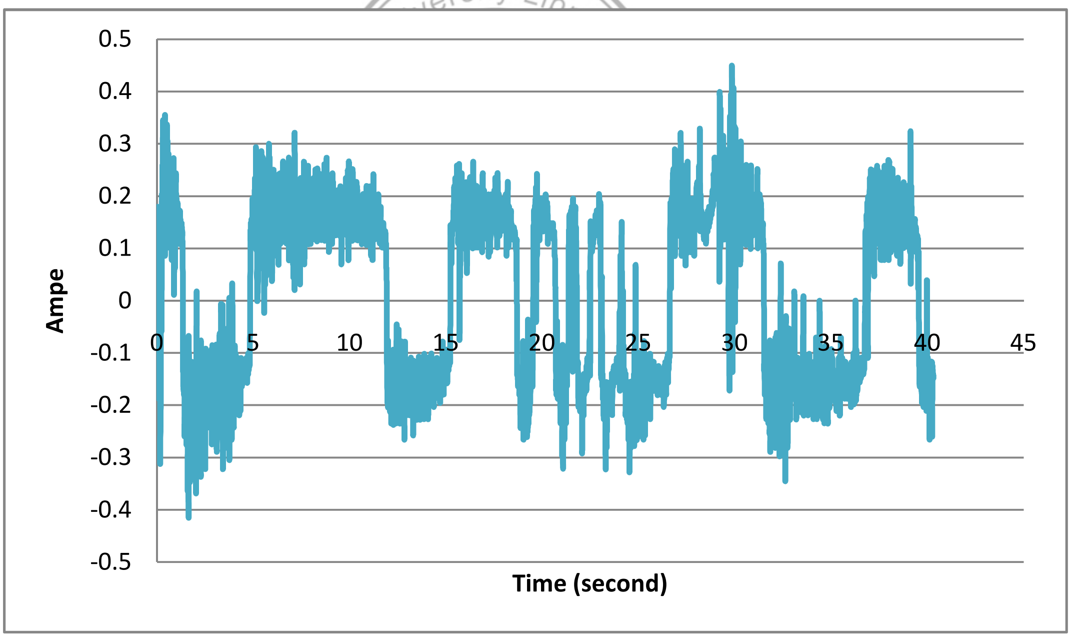

(b)

Figure 4. 34. Experimental results of conventional AFSMC at case 2

(a) Inclined angle, (b) Output current of PWR for one wheel

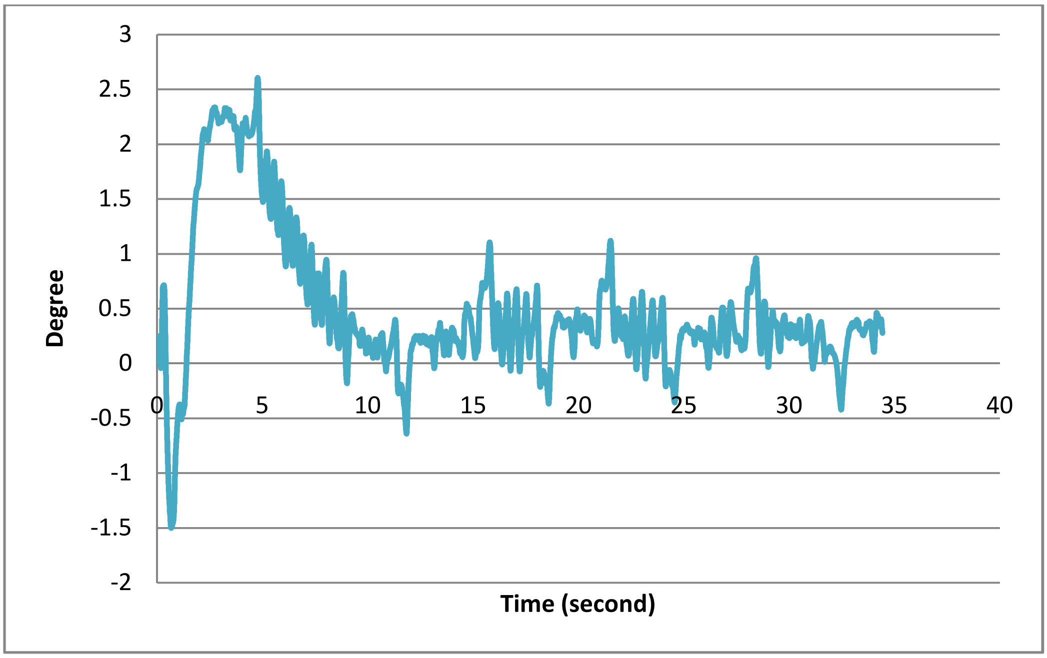

(a)

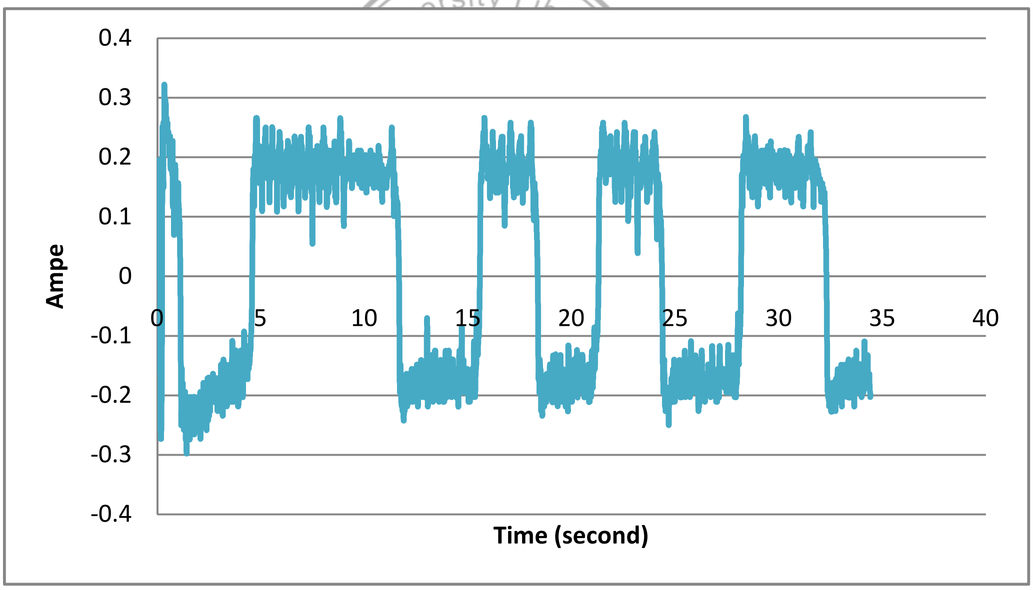

(b)

Figure 4. 35. Experimental results of proposed AFPIDSMC at case 1

(a) Inclined angle, (b) Output current of PWR for one wheel

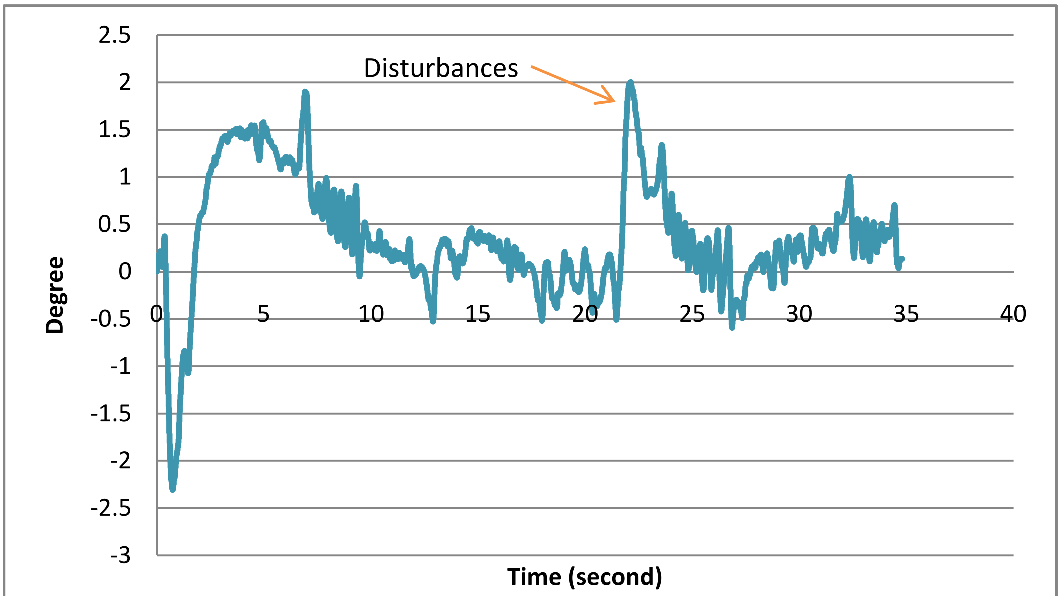

(a)

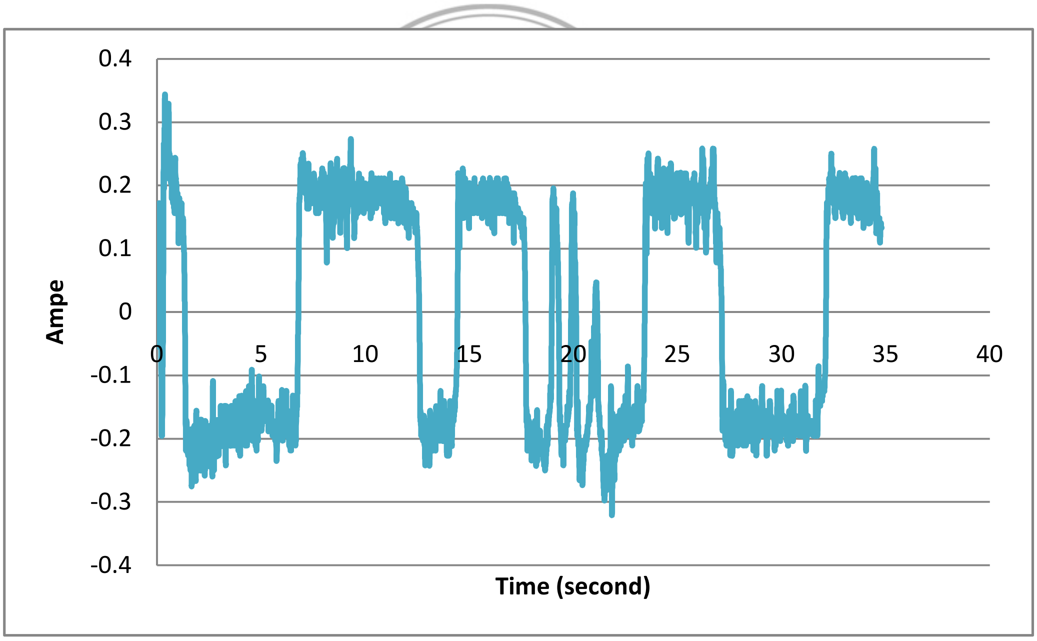

(b)

Figure 4. 36. Experimental results of proposed AFPIDSMC at case 2

(a) Inclined angle, (b) Output current of PWR for one wheel

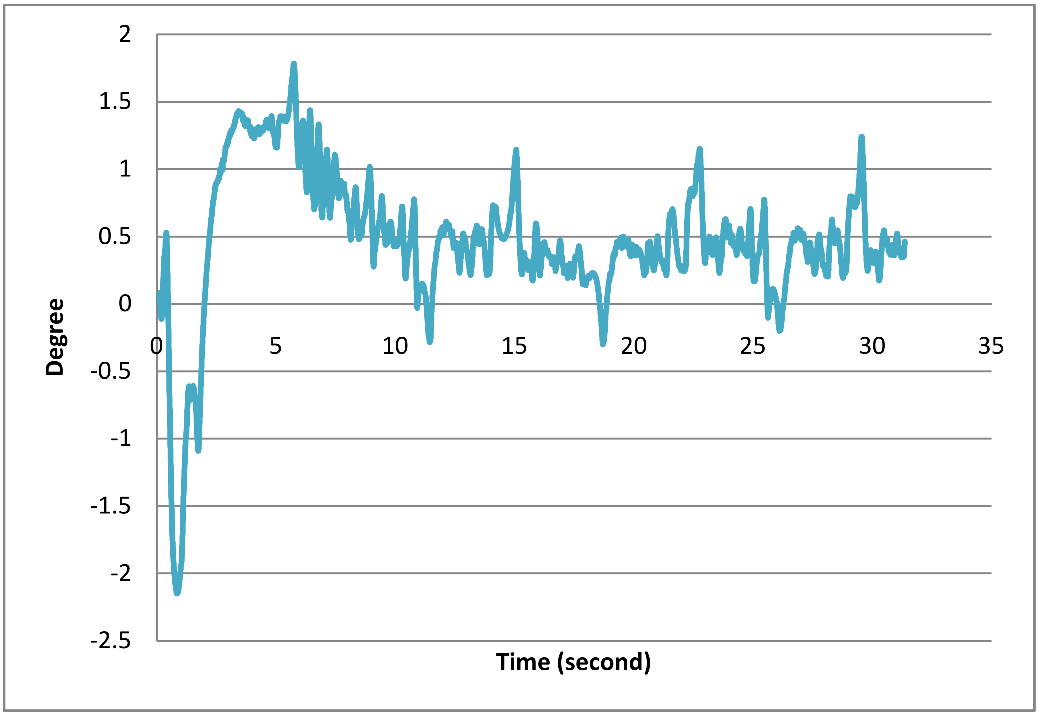

(a)

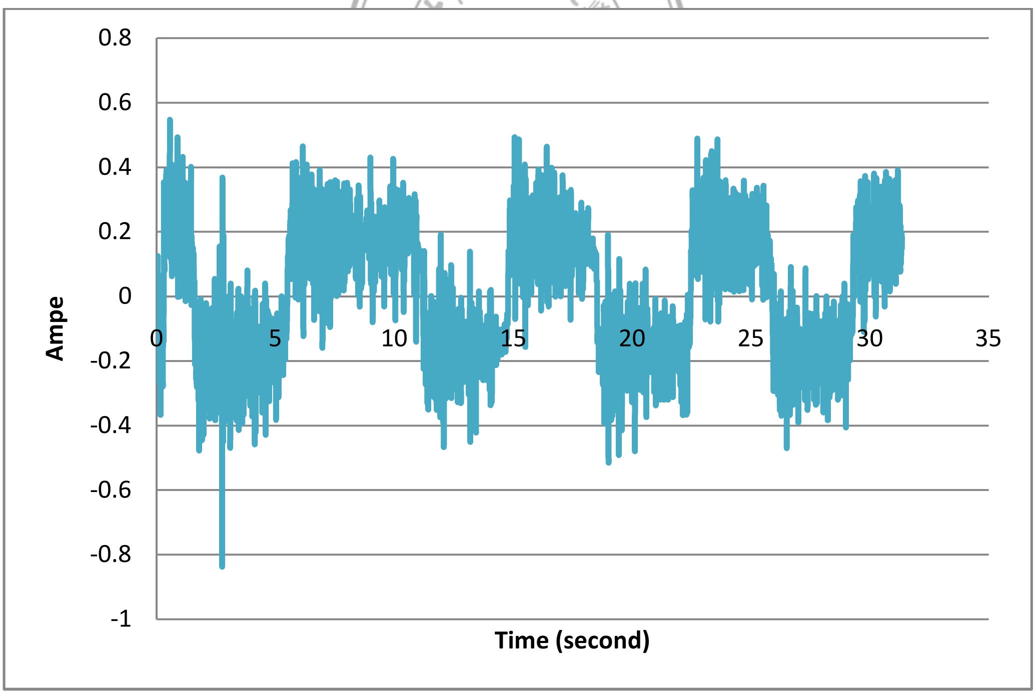

(b)

Figure 4. 37. Experimental results of conventional state feed back at case 1

(a) Inclined angle, (b) Output current of PWR for one wheel

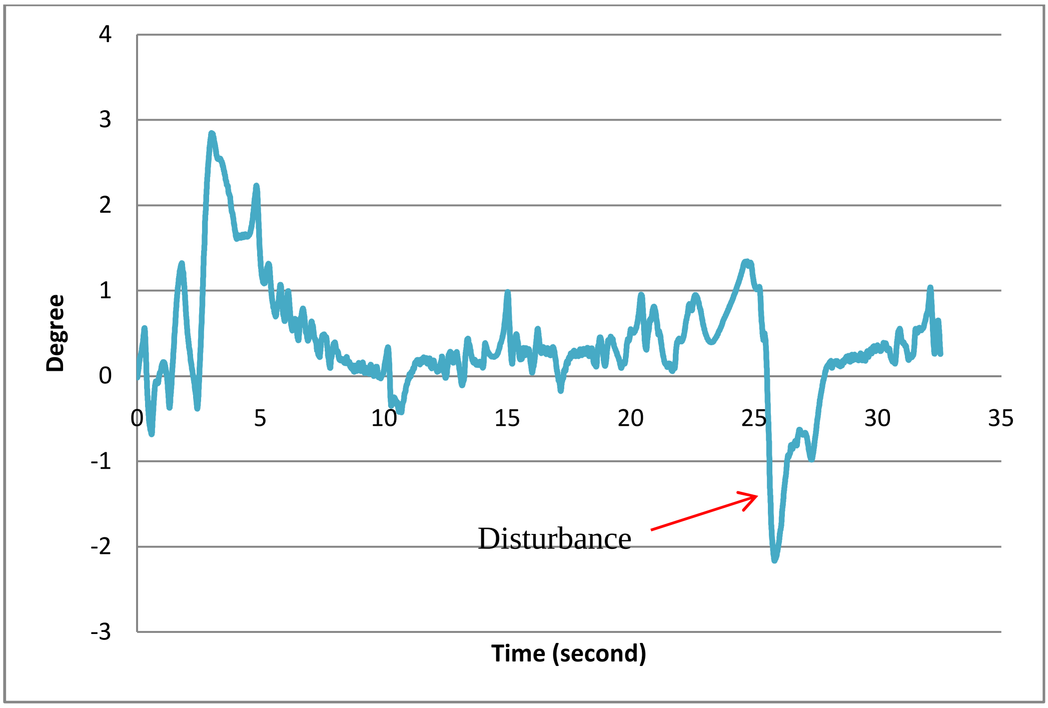

(a)

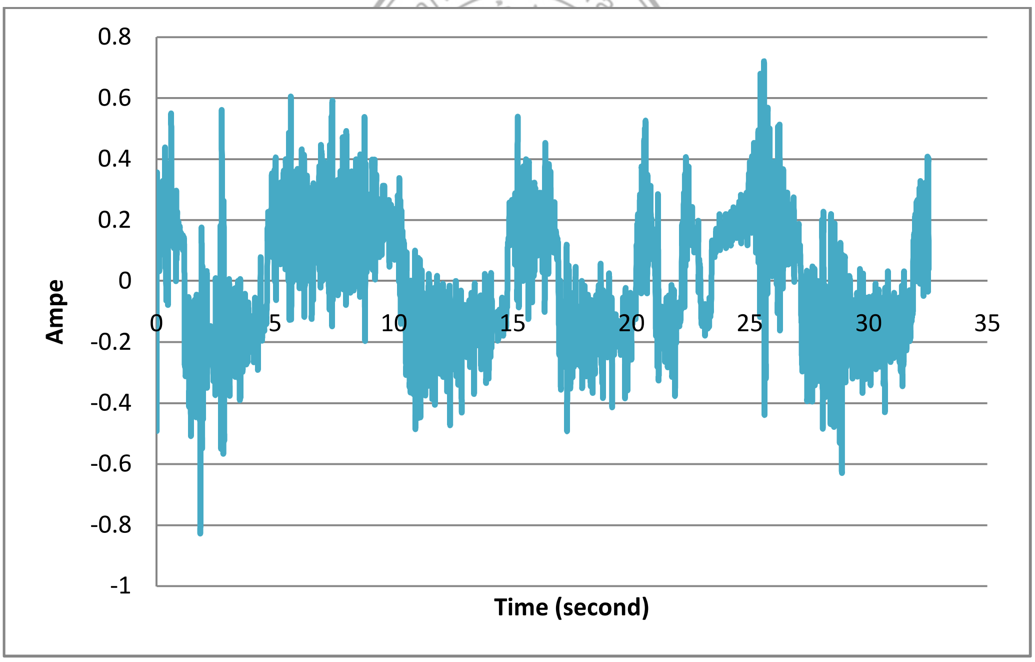

(b)

Figure 4. 38. Experimental results of conventional state feed back at case 2

(a) Inclined angle, (b) Output current of PWR for one wheel

The conventional AFSMC was considered first. From Fig. 4.33 we can see that the average value of inclined angle is approximate 0.6 degree if there is no disturbance. The control effort, or average value of the output current, is from 0.2 to 0.3 A. When disturbances appeared at the 25th second, the inclined angle was increased to 2.1 degree and the output current is changed also (Fig. 4. 34).

The performance of proposed AFPIDSMC in case 1 was shown in Fig. 4.35. The average value of inclined angle are almost 0.3 degree, and the output current is from 0.1 to 0.2 A. In case 2, even the disturbances appeared, the control effort just changed a little. Thus, we can claim that the proposed AFPIDSMC has better performance than a conventional AFSMC even the different is not so strongly.

Because the original method in E-NUVO platform is state feed back control, I also show the performance of system when applied that method in Figure 4.37 and 4.38. From the performances of three methods, we can see that the proposed AFPIDSMC has the best performance.

4.3. Discussion

The similarities between the proposed architecture and other similar schemes, e.g. conventional AFSMC, etc., are that both of them are the combination of fuzzy control, sliding mode control and adaptive tuner. This combination can not only eliminate the disadvantages of all above methods, but also have better performance than the methods which only use FC or SMC. The main disadvantage of the pure sliding mode controller is that there exists sudden and large change in the control effort during the process which leads to high stress for the system to be controlled. It also leads to chattering phenomenon of the system states. By combining SMC with FC, the change of control effort will be smoothened. On the other hand, the number of fuzzy rules in rule base is large if we just only use FC. By combining the SMC with FC, the number of rules becomes fewer and simple. In addition, by adding adaptive law into the controller, the parameter will be automatically updated to get the optimal values during the controlled period, thus the initial setting for the parameters is simple now.

The difference between the proposed architecture and other conventional AFSMCs is the definition of the sliding surface. The sliding surface included the error part and the derivative error part in conventional AFSMC while one in the proposed AFPIDSMC not only included above parts, but also included the integral part. By adding more integral element, the SMC part in controller has effectiveness even when the error is too small that can not affect error part, or the error take a long time to change that can not affect derivative part. Thus the steady error of system will be eliminated, the system will be more stable and the precision of the controller, which is very important in tracking controller, will be improved.

CHAPTER 5

CONCLUSIONS

In this thesis, an AFPIDSMC is proposed to attenuate the effects caused by un-modeled dynamics, disturbance and approximate error, for nonlinear dynamic system. The design principle is that a novel reinforced adaptive mechanism and the PIDSMC technique are incorporated into the fuzzy controller to strengthen its anti-disturbance ability. The proposed method possesses the advantages that it behaves like PIDSMC, can reduce the fuzzy rules like FSMC and can automatically adjust the membership function like AFC. In this study, the adaptive techniques are applied to the design of the stable fuzzy controller.

This thesis has also demonstrated two application examples of the proposed scheme. One is application to steer the wheeled robot with simulation results, other is application to inverted pendulum with both simulation results and experimental results. Performance comparisons of the conventional AFSMC and proposed AFPIDSMC systems are carried out in this paper. From the results, it shows that the proposed AFPIDSMC yields superior control performance than the conventional AFSMC scheme.

REFERENCES

[1] K. J. Astrom and B. Wittenmark, *Adaptive control*, New York: Addison-Wesley, 1995.

[2] J. E. Slontine and W. Li, *Applied nonlinear control*, New Jersey: Prentice-Hall, 1991.

[3] L. X. Wang, *A course in fuzzy systems and control*. New Jersey: Prentice-Hall, 1997.

[4] S. C. Tong, N. Sheng, and Y. M. Li, “Adaptive fuzzy control for nonlinear time-delay systems with dynamical uncertainties,” *Asian Journal of Control*, vol. 14, pp. 1589-1598, Nov. 2012.

[5] L. K. Wong, F. H. F. Leung, and P. K. S. Tam, “A fuzzy sliding controller for nonlinear systems,” *IEEE Trans., Industrial Electronics*, vol. 48, pp. 32-37, Feb. 2001.

[6] B. A. Elsayed, M. A. Hassan, and S. Mekhilef, “Decoupled third-order fuzzy sliding model control for cart-inverted pendulum system,” *Applied Mathematics & Information Sciences*, vol. 7, pp. 193-201, Jan. 2013.

[7] C. W. Tao, M. L. Chan, and T. T. Lee “Adaptive fuzzy sliding mode controller for linear systems with mismatched time-varying uncertainties,” *IEEE Trans., Systems, Man, and Cybernetics, Part B*, vol. 33, pp. 283-294, Apr. 2003.

[8] V. Nekoukar and A. Erfanian, “Adaptive fuzzy terminal sliding mode control for a class of MIMO uncertain nonlinear systems,” *Fuzzy Sets and Systems*, vol. 179, pp. 34-49, Sep. 2011.

[9] A. Gholami and A. H. D. Markazi, "A new adaptive fuzzy sliding mode observer for a class of MIMO nonlinear systems," *Nonlinear Dynamics*, vol. 70, pp. 2095-2105, Nov. 2012.

[10] R. J. Lian, "Design of an enhanced adaptive self-organizing fuzzy sliding-mode controller for robotic systems," *Expert Systems with Applications*, vol. 39, pp. 1545-1554, Jan. 2012.

[11] D. Chwa, "Fuzzy adaptive tracking control of wheeled mobile robots with state-dependent kinematic and dynamic disturbances," *IEEE Trans., Fuzzy Systems*, vol. 20, pp. 587-593, June 2012.

[12] C. Liu, X. H. Huang, and M. Wang, "Target tracking for visual servoing systems based on an adaptive Kalman filter," *Int. Journal of Advanced Robotic Systems*, vol. 9, DOI: 10.5772/52035, Oct. 2012.

[13] K. H. Su, "Robust tracking control design and its application to balance a two-wheeled robot steering on a bumpy road," *Proc. Inst. Mech. Eng., Part I: J. Syst. & Control Eng.*, vol. 226, pp. 887-903, Aug. 2012.

[14] A. G. Ak, G. Cansever, and A. Delibasi, "Robot trajectory tracking with adaptive RBFNN-based fuzzy sliding mode control," *Information Technology and Control*, vol. 40, pp. 151-156, 2011.

[15] R. J. Wai and K. H. Su, "Adaptive enhanced fuzzy sliding-mode control for electrical servo drive," *IEEE Trans., Industrial Electronics*, vol. 53, pp. 569-580, Apr. 2006.

[16] I. Zohar, A. Ailon, and R. Rabinovici, "Mobile robot characterized by dynamic and kinematic equations and actuator dynamics: Trajectory tracking and related application," *Robotics & Auton. Syst.*, vol. 59, pp. 343-353, June 2011.

[17] M. Elie, S. Maarouf, and S. Hamadou, "A higher level path tracking controller for a four-wheel differentially steered mobile robot," *Robotics & Auton. System*, vol. 54, pp. 23-33, Jan. 2006.

[18] J. O. Jang, "Adaptive neuro-fuzzy network control for a mobile robot," *J. Intel. Robot System*, vol. 62, pp. 567-586, June 2011.

[19] Choi S-B, Ham JH, Nguyen, VQ, et al. A new perturbation estimator in a sliding mode control system with application to robot control. *Proc IMechE, Part I: J Systems and Control Engineering 2008*; 222(6): 425–435.

[20] Wang L-X. Adaptive fuzzy systems and control. Englewood Cliffs, NJ: Prentice-Hall, 1994.

[21] Yang H, Yang SX and Mittal GS. Tracking control of a nonholonomic mobile robot by integrating feedback and neural dynamics techniques. *In: IEEE/RSJ international conference on intelligent robots and systems (IROS2003), MC Lin (ed), Las Vegas, NV, 27–31 October 2003, pp.3522–3527.* Chapel Hill: University of NorthCarolina.